CHAPTER 2

LITERATURE REVIEW

To identify the suitability of all the indirect incorporation methods of the PCM in the building envelope, to improve the indoor thermal behavior, a detailed literature review is needed. Therefore, this chapter presents a detailed and robust literature review on all the three types of indirect incorporation techniques of PCM in the building envelope. In section 2.1, discussion on Microencapsultaed PCM (mPCM) and its application in improving indoor thermal comfort of the building is presented. Section 2.2 contains detailed literature review on Macroencapsulated PCM (MPCM) and its application in improving indoor thermal behavior of the building. Section 2.3 discusses about shape stabilized composite PCM (ss-CPCM) technique and its effectiveness in improving building energy efficiency.

2.1 Microencapsulation

Microencapsulation is the process of enclosing the micron size particles of solid, liquid and gasses in an inert shell. The Microencapsulated PCM (mPCM) are the very tiny sized particles, having PCM nucleus inside the protective layer as shown in Figure 2.1. The shell will act as a protective layer and protects the particles from the external environment.

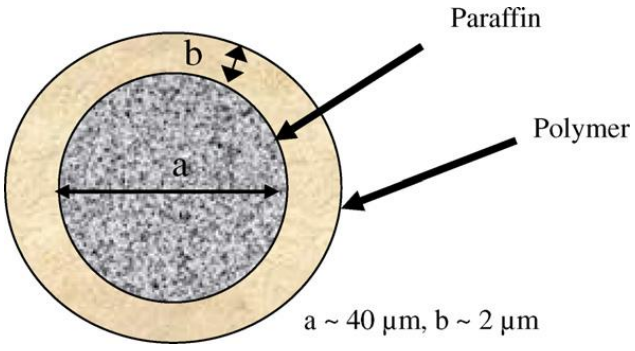

Figure 2.1 Microencapsulation of paraffin as core material having polymer shell (69)

The PCM changes its phase inside the protective shell as per the prevailing thermal condition thus, reducing the chances of leakage and any type of chemical and physical reaction with the external environment. The mPCM has various advantages such as an increased surface area for heat transfer, no leakage, reduced reactivity of PCM towards the external environment and controlling the phase change process (70). The process of heat gain and heat loss by the PCM, inside a capsule shell is shown in the Figure 2.2. Initially, the PCM is in solid state inside the capsule and as soon as the temperature rises the PCM absorbs the heat energy and consequently, it liquefied. When the temperature falls, the liquid PCM inside the capsule releases heat energy to the surrounding resulting in the solidification of the PCM.

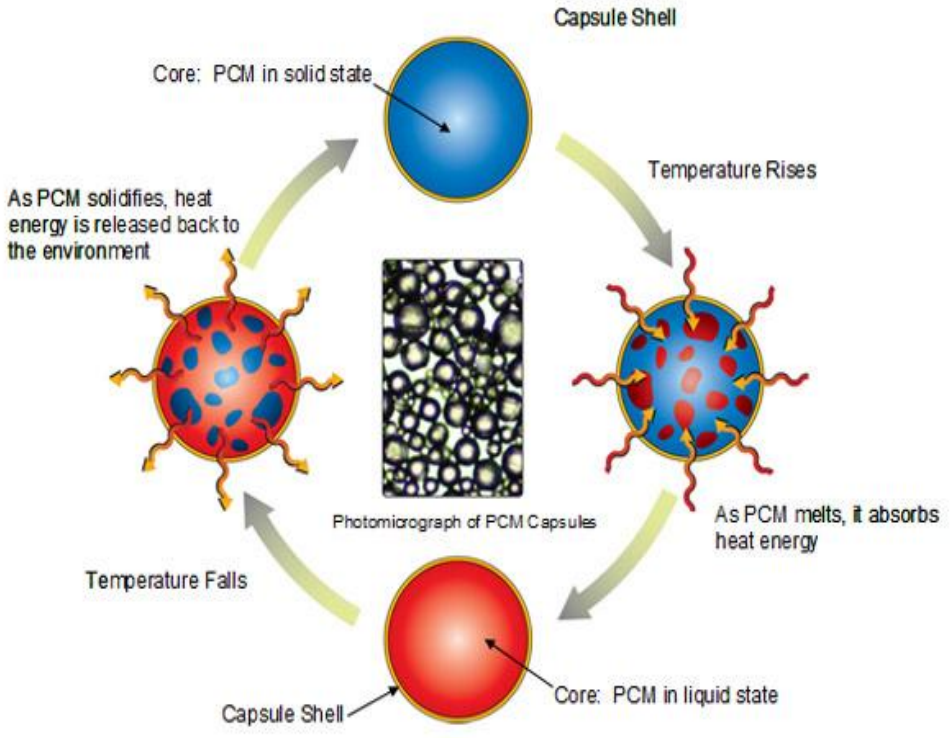

Figure 2.2 Energy gain and loss using mPCM (71)

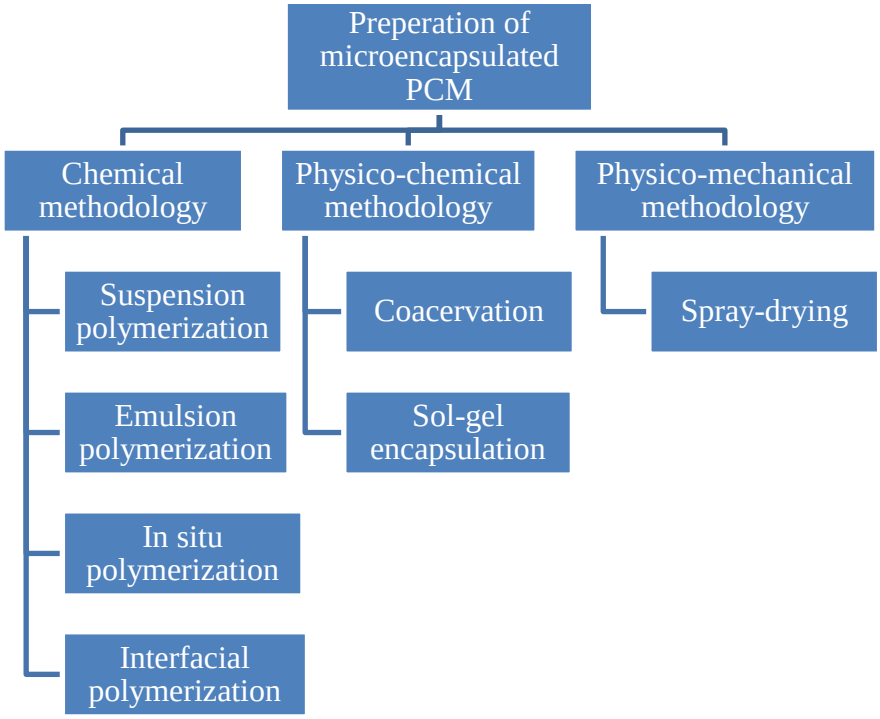

Figure 2.3 Methods of preparation of mPCM (72)

There are several techniques available for the preparation of mPCM. A broad classification is shown in Figure 2.3. The detailed study of these techniques is available in literature (73,74). However, a few characteristics of the mPCM, produced by these techniques are summarized in Table 2.1. The encapsulation ratio is one of the most important parameter which affects the heat transfer characteristics of the mPCM. It indicates the effectiveness of the PCM inside the shell and is calculated using the following relation (75).

$$E.R = \frac{(\Delta H)_{mpcm}}{(\Delta H)_{pcm}} \times 100 \qquad (1)$$

Where, $(\Delta H)_{mpcm}$ is the latent heat of the mPCM and $(\Delta H)_{pcm}$ is the latent heat of the PCM. The encapsulation depends on the thickness of the shell material, the thicker the shell the lower is the encapsulation ratio. mPCM with a higher encapsulation ratio is preferred for thermal energy storage. Reduced particle size of mPCM will increase the encapsulation ratio and thus also increases the effectiveness of the mPCM.

Table 2.1 Characteristics features of MPCM techniques

Microencapsulation Technique	Particle Size (μm)	Encapsulation ratio	Shell material	Commonly used PCM
Suspension polymerization	2-4000	7-75	Octadecyl methacrylate-methacrylic acid, butyl methacrylate	Paraffin wax
Emulsion polymerization	0.05-5	14-67	Polystyrene, Polymethyl methacrylate(PMMA)	Paraffin wax, Palmitic acid
In situ polymerization	1-2000	43-95	Poly (ethyl methacrylate), PMM	Dodecanol, Paraffin wax
Interfacial polymerization	0.5-1000	15-88	Polyurethane Urea, formaldehyde Melamine, formaldehyde	Paraffin wax
Coacervation	2-1200	6-68	Formaldehyde resin, Gelatin	Paraffin wax, Octanoic acid
Sol-gel encapsulation	0.2-20	30-87	SiO_2, TiO_2	Paraffin wax, Stearic acid
Spray-drying	0.1-5000	38-63	TiO_2, Gelatin	N-octadecane, Paraffin wax

Another important parameter which affects the heat transfer characteristic of mPCM is encapsulation efficiency (η_{encap}). It can be derived from the following relation (76).

$$\eta_{encap} = \frac{\Delta H_{m,mpcm} + \Delta H_{c,mpcm}}{\Delta H_{m,pcm} + \Delta H_{c,pcm}} \times 100 \qquad (2)$$

Where, $\Delta H_{m,pcm}$ and $\Delta H_{m,mpcm}$ are the melting enthalpies of the pure PCM and mPCM respectively and $\Delta H_{c,pcm}$ and $\Delta H_{c,mpcm}$ are the crystallization enthalpies of the pure PCM and mPCM respectively. A higher encapsulation efficiency of the mPCM is required because it gives high mechanical strength and leak proof characteristics. Shell material also plays an important role in deciding the performance of the mPCM. A highly reliable shell material

will ensure good thermal performance along with high mechanical strength of the mPCM. An ideal shell material should fulfill the following criteria.

1. It should have high mechanical and thermal strength to withstand at high transition temperature of the PCM.

2. It should be inert so that it doesn't react with the PCM and causes undesirable chemical changes.

3. It must have high thermal conductivity to improve the heat transfer from the PCM to the surroundings.

4. It must retain all its thermo-physical characteristics at micro/nano level

5. It must have good anti-osmosis properties to ensure a longer lifespan.

6. It must be leak proof

The weight ratio of the PCM to the whole capsule was determined by using below given relation:

$$\frac{m_{pcm}}{m_{pcm} + m_{shell}} = \frac{\frac{4}{3}\pi.R_{pcm}^3 .\rho_{pcm}}{\frac{4}{3}\pi.R_{pcm}^3 .\rho_{pcm} + \frac{4}{3}\pi.(R^3 - R_{pcm}^3)\,\rho_{shell}} \qquad (3)$$

$$= \frac{1}{1+\left[\left(\frac{R}{R_{pcm}}\right)^3 - 1\right]\left(\frac{\rho_{shell}}{\rho_{pcm}}\right)} \qquad (4)$$

Where, capsule radius R is the sum of the core PCM radius, R_{pcm}, and shell thickness. With determined capsule radius and weight ratio and known densities of core and shell materials, R_{pcm} can be determined from equation (4). A wide range of materials are used to encapsulate the PCM at the micro level. Most commonly used materials are organic material, inorganic material composite/hybrid material, and bio-based material.

mPCM are widely used in textile industries, food and beverage industries and pharmaceutical industries for various applications. The application of mPCM in the building

industry is quite new and attracted many researchers to evaluate the performance of the building envelope by integrating mPCM with the building material. Due to their ability to improve the thermal performance in various applications, lots of mPCM are readily available in the market. These mPCM are known by their commercial names. A list of various commercial manufacturers of the mPCM across the globe is summarized in Table 2.2.

Table 2.2 List of manufacturers of MPCM

Trademark name	Country of origin	Official website	Particle size
Microtek Laboratories, Inc.	USA	www.microteklabs.com/	14-24 µm
Rubitherm technologies	Germany	www.rubitherm.eu/	10-20 µm
Pure temp LLC	USA	www.puretemp.com/	10-1000 µm
Shanghai Tempered Entropy New Energy Co.	China	www.chinapcm.com/profile	≤10µm
MikroCaps	Slovenia	www.mikrocaps.com/	--
Winco technologies	France	www.wincotech.com/en/home/	5-50 µm

2.1.1 mPCM integrated in building material

Incorporation of mPCM in the building material ensures effective heating and cooling of the PCM because of the direct exposure of the building walls and roofs to the solar radiation. Therefore, to maintain the indoor thermal comfort, mPCM can be directly

used in the building walls and roofs to enhance the thermal energy storage capacity of the buildings (77).

mPCM intertek 23°C, purchased from MCI Technologies, was integrated with the textile reinforced concrete panel in varying proportions (0%, 15%, and 20%) and was evaluated for thermal energy storage behavior by (78). Figure 2.4 (a) shows the laboratory experimental setup of the prepared mPCM-textile reinforced concrete panel and Figure 2.4 (b) shows the real outdoor weather testing setup of the prepared concrete panel. The laboratory result indicates that the integration of the mPCM leads to a reduction of thermal conductivity of the concrete panel. For 20% sample of the concrete panel, the thermal conductivity reduces to 46% in comparison to the panel without mPCM. The amount of stored heat and latent heat, both, increases as the percentage of mPCM is increased. Real outdoor testing shows shifting of the peak to 2 hours with night ventilation.

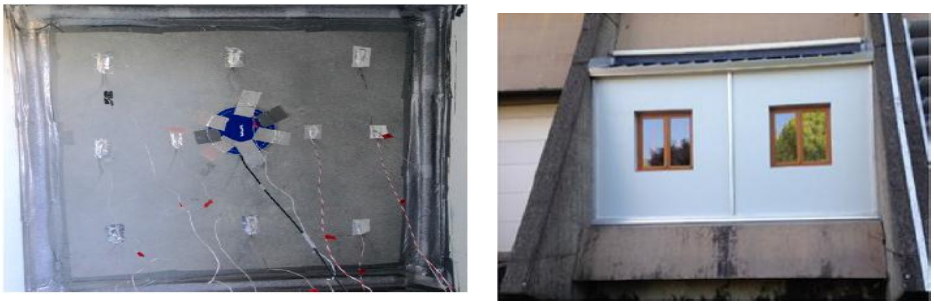

(a) (b)

Figure 2.4 (a) Textile reinforced concrete panel with MPCM (b) Real weather testing (78)

The (79) have constructed two identical cubicles of dimensions 2 × 2 × 3 m, as shown in Figure 2.5. One of the cubicle is having mPCM called micronel PCM (in south, west and roof walls), which is having a phase change enthalpy of 110 kJ/kg and a melting temperature of 26°C while the other cubicle is without PCM. A time lag of 2 hours in the

heat wave and a peak temperature difference of 3°C have been achieved in the cubicle having mPCM. They have conducted two more experiments on the same cubicles by opening and closing the window to investigate the effect of free cooling. The free cooling effect has further reduced the temperature difference between both the cubicles.

Figure 2.5 Developed cubicles using MPCM for analysis (79)

Thermal performance of two-full size test rooms, one integrated with mPCM plaster and the other integrated with reference plaster, was evaluated by (80). Rooms were tested for two consecutive years with two different mPCM. For one year, the dispersion-based plaster with 40wt% PCM and 6 mm of thickness was tested and for the second year, the gypsum plaster with 20wt% PCM and 15 mm thickness was used. Figure 2.6 (a) shows schematic of the lightweight wall of the full-size test rooms and Figure 2.7 (b) shows the test rooms at Fraunhofer ISE façade testing facility. Following test results were obtained:

(a) The temperature rise is slow in the room with PCM, in comparison to the room without PCM.

(b) A time lag in attaining maximum temperature is achieved in the room with PCM

(c) The room without PCM has recorded a temperature above 28°C for more than 50 hours, whereas the room with PCM has recorded a temperature above 28°C for only 5 hours for a testing time-period of 3 weeks.

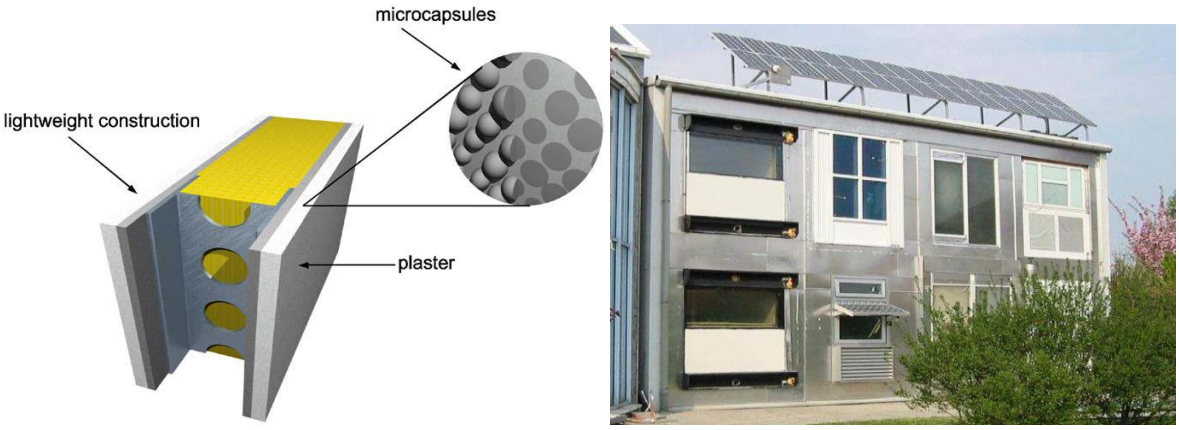

Figure 2.6 (a) Schematic of lightweight PCM wall (b) Full-size test room at Fraunhofer ISE (80)

Effect of adding awnings on the indoor thermal behavior of the test rooms, which are having mPCM (Micronal PCM) integrated with the building material, was evaluated by (81). Two cubicles of sizes 2.64m × 2.64m × 2.52m were erected as shown in Figure 2.7. One cubicle is developed without using mPCM while the other one is developed by integrating mPCM capsules.

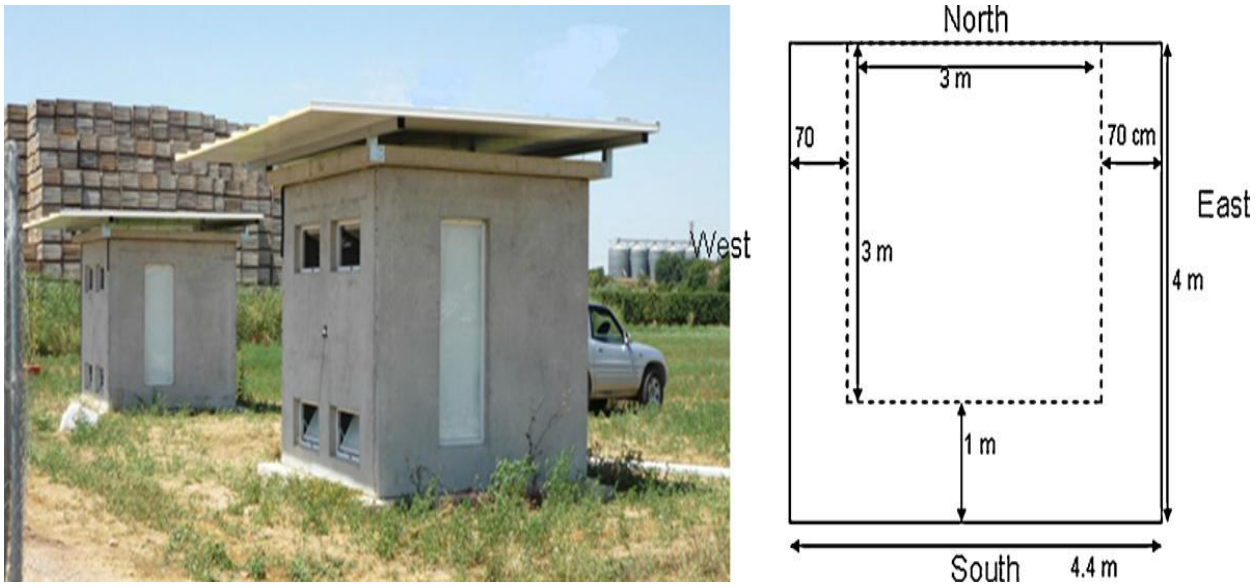

Figure 2.7 Full size test room with and without MPCM on left and schematic of test room on the right (81)

The east wall and the west wall are having one window each of dimension of 1.7m × 0.6m and the south wall is having four windows of dimensions 0.75m × 0.4m. North wall of the cubicles is having a door. It has been analyzed that peak temperature reduction was increased by 6% and the time of the indoor thermal comfort was also increased between 10% to 21%. A time lag of more than 30% in attaining maximum temperature was also observed in the cubicle having mPCM.

Nine small house-sized cubicles of dimensions 2.4 × 2.4 × 2.4 m were erected (82) to observe the effect of integrating mPCM directly into the concrete and bricks. All the nine cubicles were identical, but they are built using different construction materials. Cubicle 1 is made by using only concrete and no insulation, cubicle 2 is made by using concrete with mPCM and with no insulation, cubicle 3 is made by using brick with no insulation, cubicle 4 is made by using brick and 5 cm of polyurethane, cubicle 5 is made by using brick with 5cm of polyurethane and mPCM, cubicle 6 is made by using brick and 5cm of polystyrene,

cubicle 7 is made by using brick with 5cm of mineral wool, cubicle 8 is made by using alveolar brick and cubicle 9 is made by using alveolar brick with mPCM. Free cooling and controlled temperature experiments were performed in all the cubicles. The results show that the maximum temperature of the concrete cubicle having mPCM is 1°C lower than the cubicle without mPCM and a time delay of 2 hours is also achieved by mPCM cubicle. The brick cubicles having mPCM have obtained almost 15% and 17% of improvement in energy savings in comparison to brick cubicles without mPCM.

In (83), varied percentage (0%, 10%, and 20%) of microcapsules was integrated with two different types of single layer mortar and tested for thermal, mechanical and fire behavior. Micronal DS5001 microencapsulated paraffin PCM, having a melting point of 26°C and latent heat capacity of 146 kJ/kg was used. Experimental results show that the thermal conductivity and diffusivity decreases with the increase in the content of the mPCM in the mortar. An increase in the percentage of mPCM increases the specific heat capacity by 22.5% and 28% of samples containing 10% and 20% of mPCM respectively. The authors also concluded that the inclusion of mPCM in the mortar reduces its compressive strength.

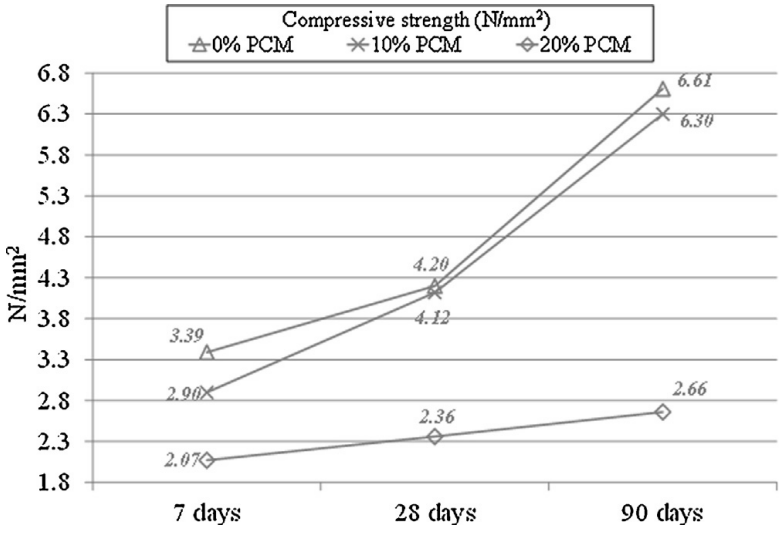

Figure 2.8 Compressive strength of prepared mortar-PCM samples (83)

Figure 2.8 describes the change in the compressive strength of prepared samples after 7 days, 28 days and 90 days of the hydration time period. The best results were shown by 10% of mPCM, which has 1.90% of decrement in compressive strength, in comparison to sample without mPCM. A composite mPCM system was developed by (84) and is tested for indoor thermal behavior of high rise buildings having 80% window to wall ratio. The Energain PCM panel and Bio PCM panel having a melting temperature of 21°C and 25°C are used to integrate into the test cell as shown in the Figure 2.9. The test cells were constructed using an aluminum structural frame covered with white rigid polyethylene plastic sheet and was provided with extruded polystyrene insulation. The results predict a reduction in temperature fluctuation as well as in peak temperature. The variation in ambient weather condition (Fall month and summer month) has been effectively taken care by the composite PCM system because Energain layer will improve the indoor thermal behavior during the fall month whereas BioPCM will improve the indoor thermal behavior during the summer month. This type of the composite system is very useful for the locations having a high diurnal temperature range.

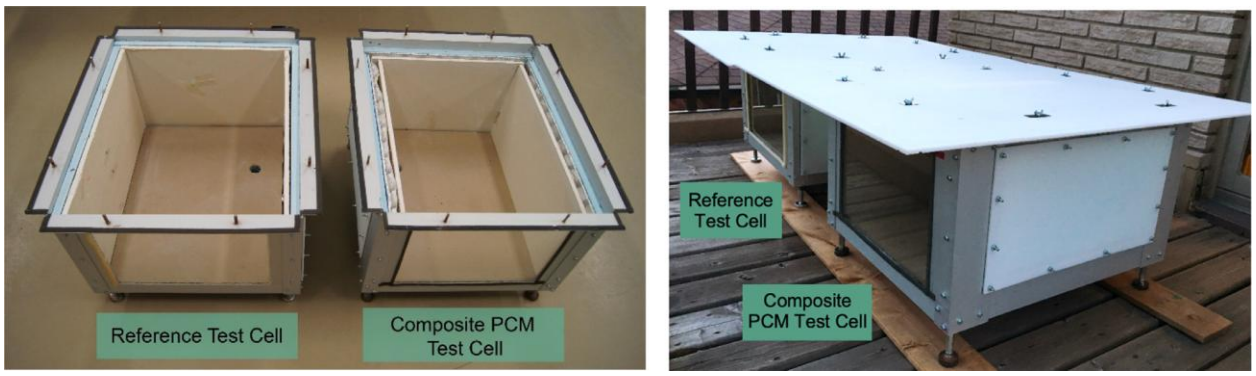

Figure 2.9 Developed reference test cell and composite PCM test cell (84)

In a recent study (85), a eutectic PCM containing capric acid and mystric acid (75:25 wt%) was used to develop mPCM into a polystyrene shell by using emulsion polymerization technique.

(a)

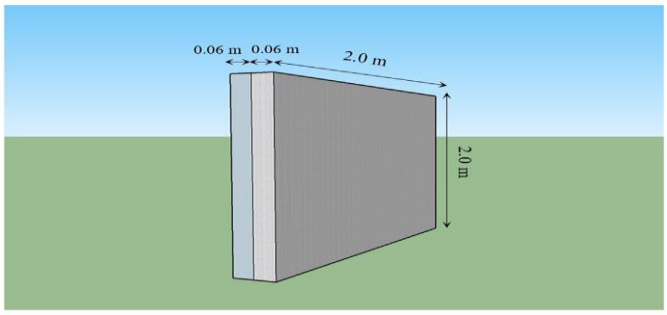

Figure 2.10 (a) Developed test buildings under outdoor environment condition (b) Fabricated composite panel (85)

These mPCM was then integrated into the concrete and was used to fabricate composite concrete panels of dimensions 2 × 2 × 0.12 m, as shown in Figure 2.10 (b), these panels were then used to develop two identical building structure, one with mPCM panel and the other without mPCM panel, as shown in the Figure 2.10 (a). The results show a reduction of 2˚C at noontime which leads to 13% of energy savings. Due to the presence of mPCM, 5˚C of temperature difference is visible between mPCM building and reference building. However, a reduction in mechanical strength was also observed due to the mixing of mPCM in the concrete.

Wallboards, gypsum, and plasterboards are one of the most widely used materials for interior walls and ceilings of a building structure. These materials are also commonly used

for retrofitting of the buildings. Therefore, there is also a need to optimize the thermal performance of these types of materials. In (86), mPCM is integrated with aluminum honeycomb structures to construct a PCM honeycomb wallboard prototype of height 10 cm, length 10 cm, and width 2.54 cm. The results suggest that PCM wallboard possessed sufficient heat conduction enhancement and time lag of the peak load. This prototype performs well for the control of the surface temperature. Another prototype of mPCM honeycomb wallboard (30 cm × 30 cm × 3 cm) is analyzed by (87), for the thermal behavior when the outdoor side of the wallboard is exposed to the solar radiation and the indoor side is subjected to the forced and natural convection. It has been found that indoor condition influences the thermal behavior of the PCM honeycomb wallboard. If the indoor conditions are subjected to the forced or natural convection then the PCM can effectively release the heat. The maximum thermal protection period of 4.7 hours and heat-releasing period of 3.8 hours is achieved using the PCM honeycomb wallboard.

A composite timber wall consists of timber, vacuum insulation panel, and microencapsulated PCM is prepared and optimized by (88), as shown in Figure 2.11. The PCM used here is a polymer-paraffin compound in an aluminum panel having a latent heat of 70 kJ/kg. A time lag of almost 9 hours to 12 hours in heat wave propagation was achieved. Additionally, night time heat loss is 90% lower than the normal timber wall.

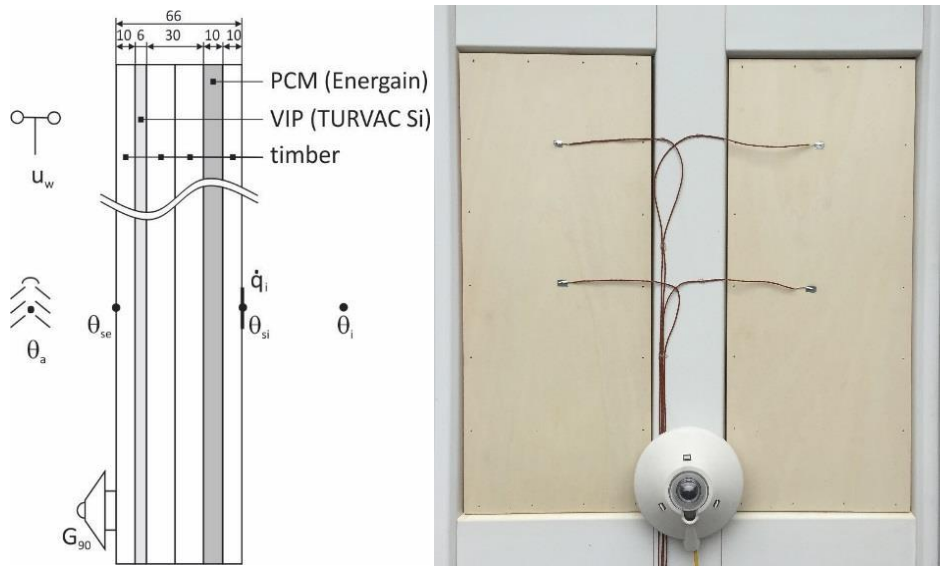

Figure 2.11 Sectional view (Left) of composite timber and experimental setup outside view (Right) (88)

Perforated plasterboard incorporated with commercially available mPCM, the micronal DS 5001, from BASF was prepared as shown in Figure 2.12 and tested for the thermal behavior by (89).

Figure 2.12 Perforated MPCM plasterboard with holes (89)

The mPCM has a melting temperature of 26°C and latent heat capacity of 110 kJ/kg. The test results indicate that there is an increase of 9.5% in absorbing heat flux of prepared plasterboard in comparison to normal plasterboard. It has been observed that making holes in PCM plasterboard increases the temperature swing of the internal surface. The absorption and release of the heat flux increase with the decrease in the spacing of holes. They have also concluded that the reduction in the spacing of the holes will lead to an increase in phase shift at an average time of 3.5 hours. A gypsum PCM board was developed by using gypsum powder and mPCM with a mass fraction of 30% by (90). The melting temperature of the mPCM is 25.8°C. The dimension of the tested component is 0.35 × 0.35 × 0.3 m as represented in Figure 2.13. The prepared product is tested in a testing chamber having temperature monitoring equipment, air temperature control device and air velocity control device.

Figure 2.13 Gypsum powder, MPCM and prepared gypsum-MPCM panel (90)

Following are the conclusions that authors have made:

(a) Reduction in phase change period and increment in the phase change rate was observed when air temperature and air velocity increases.

(b) Heat flux change rate and the peak value increase with the increase in the air velocity and the temperature.

(c) Opening and closing of the ventilation system must be at the proper time to increase the energy savings.

(d) The energy savings will be maximized if the air temperature is maintained at 40°C, the air velocity at 1.5 m/sec and the ventilation time is 2.4 hours.

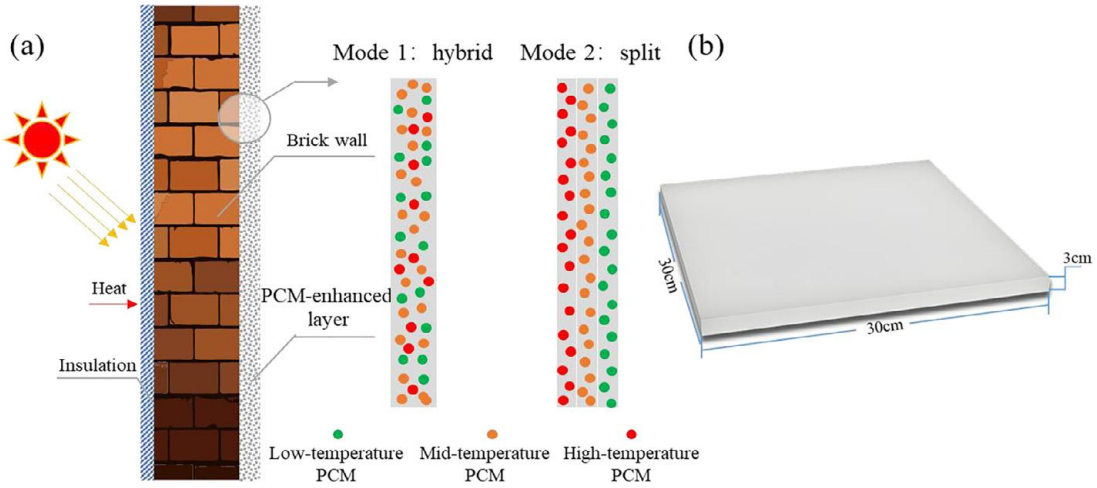

Figure 2.14 (a) New combination of hybrid PCM gypsum wallboard (b) Dimension of gypsum wallboard (91)

A latest study (91) suggest the use of hybrid PCM wallboard for improving energy efficiency and thermal comfort in the building. Three different types of mPCM namely, mPCM-12, mPCM-18, and mPCM-29 having melting temperature of 12˚C, 18˚C and 29˚C respectively were used. These PCM were integrated into the gypsum wallboard in two different modes and are compared for thermal behavior with the ordinary gypsum wallboard. In mode 1 the mPCM are directly combined with the gypsum wallboard whereas, in mode 2 three different layers of mPCM are combined with gypsum wallboard, as shown in the Figure 2.14 (a) and 2.14 (b). The results indicate that the mode 2 is more suitable for

delaying the heat transfer from outdoor to indoor and for discharging of mPCM in comparison to mode 1. The author has concluded that these types of hybrid systems are more adaptable to seasonal variation in comparison to single layered mPCM gypsum wallboard.

The analysis of incorporating the mPCM in the lightweight building structures/materials suggests that the mPCM is compatible with lightweight structures like plasterboard, wallboard, gypsum, etc. These lightweight structure integrated with mPCM can also be used as a retrofitting in older buildings. Additionally, the mPCM significantly improves the thermal energy storage capacity of the lightweight building materials and also improve the thermal regulating behavior of the components. However, one of the limitations of mPCM technology in comparison to macroencapsulation or Shape stabilized PCM is the price of mPCM. As per National Renewable Energy Laboratory (NREL, USA) the cost to macroencapsulate a PCM is ~20% of the total cost whereas to microencapsulate a PCM almost ~50% of the final product cost is required (92). An increase in the final price of the MPCM creates a bottleneck for the growth and development of this technology. However, the final cost of the product significantly depends on the type of the PCM (Organic, Inorganic, and Eutectics) used for encapsulation. Among all the available PCMs, commercially available paraffinic PCMs are much cheaper because they are the by-product of oil refineries and therefore are available in abundant supply. PCM product cost is primarily governed by the cost of the raw PCM material and the cost of encapsulation. The final PCM product cost varies greatly depending on the approach adopted to encapsulate the PCM.

Therefore, it can be concluded that encapsulating the PCM in microcapsules will not only reduce the chances of leakage during phase transition but also improves the heat transfer

characteristics of the PCM. Polymers, both synthetic and natural, are commonly used as a shell material to microencapsulate the PCM. However, some other material with good heat transfer rate can also be used as a shell material.

2.2 Macroencapsulation

Macroencapsulation of the PCM is the process of encapsulating the PCM in the shell material having a size of more than 1mm. There are different definitions of macroencapsulation given in terms of size and/or shape by various researchers. The (93) has defined macroencapsulated PCM(MPCM) with size of container of more than 1cm. The (94) has defined the macroencapsulated PCM whose size is more than 1000 μm. Similarly, (95) has also categorized the macroencapsulated PCM whose container size is more than 1mm. The (96) has defined macroencapsulation as the inclusion of PCM in some forms of packaging like tubes, pouches, panels and other receptacle having size larger than 1 cm. The shape of the encapsulating shell can be of any form (tubes, cylinders, pouches, cubes, etc.). This makes MPCM to get incorporated easily in the building envelope of any shape, size, and dimension. Various types of containers used to make MPCM is shown in the Figure 2.15.

The geometry of the container for the encapsulation of the PCM depends upon the dimension of the building material in which it is going to incorporate. Preferably, the container is made of metallic or plastic material. If high heat transfer is the requirement, then the metallic container can be used otherwise plastic containers could also be used.

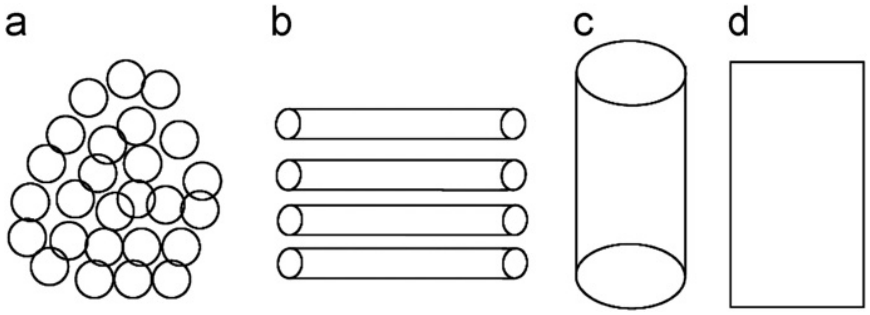

Figure 2.15 Commonly used container shape for macroencapsulation (95)

In general, the container used for encapsulation must have the following characteristics (97):

1. The material should have high thermal conductivity.
2. Must have high strength and flexibility.
3. The material should be non-toxic.
4. It should be thermally stable.
5. Should be non-corrosive and fire-resistive.
6. Should be chemically and physically stable with building material.
7. Must be stable with UV rays exposure and moisture.

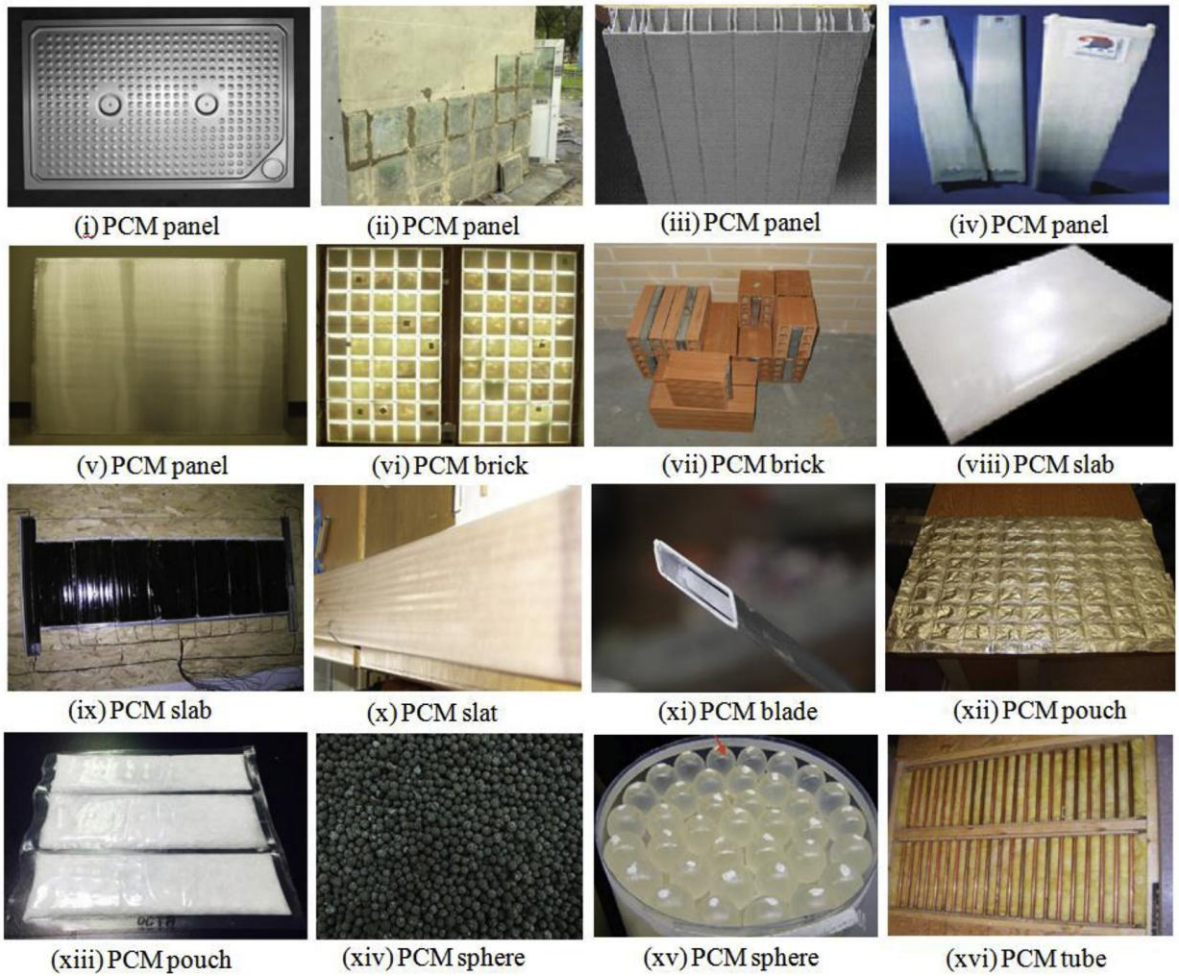

Figure 2.16 commonly used MPCM in buildings (98)

MPCM can be easily prepared in any shape and size to suit different applications as shown in Figure 2.16. Unlike microencapsulation where various methods and techniques are used to encapsulate the PCM, the macroencapsulation of the PCM doesn't require any pre-defined complicated process. Several forms of MPCM were prepared and marketed by various commercial manufacturers. The list of few renowned MPCM manufacturers and the commonly used container for macroencapsulation is shown in Table 2.3.

Table 2.3 Commercial manufacturers of MPCM

Trademark name	Country of origin	Official website	Container type
Microtek Laboratories, Inc.	USA	www.microteklabs.com/	Polymers
Rubitherm technologies	Germany	www.rubitherm.eu/	Aluminum panels, Polymer bags, Pouches.
Pure temp LLC	USA	www.puretemp.com/	Polymers, Aluminum tube, Plastic blocks, Flexible films
Shanghai Tempered Entropy New Energy Co.	China	www.chinapcm.com/profile	Polymers
MikroCaps	Slovenia	www.mikrocaps.com/	Polymers
Winco technologies	France	www.wincotech.com/en/home/	Breather membrane
Teappcm	USA	http://www.teappcm.com/	Stainless steel balls, HDPE panels, aluminum panels

The most cost effective container in the market are high density polyethylene bottles, tin-plated metal cans and mild steel cans (99). The manufacturing of the macroencapsulated PCM was done through a containment method in which the PCM is filled in some form of a container/package such as tubes, HDPE balls, spheres, pouches, metal canes, panels or other receptacles. These macrocapsules are then straight away integrated into the building elements. While preparing the MPCM, the provision for expansion due to volume change

must be considered. This is because, to cope up with the change in volume of the PCM during phase transition inside a closed packed container. Due to the change in volume there are chances of void formation which will affect the heat transfer. Various forms of MPCM was developed and incorporated in the building envelopes by researchers in recent years to investigate the potential of MPCM in improving the indoor thermal profile of the buildings.

2.2.1 MPCM embedded directly in the construction material

The (100) has developed three similar wall specimen (M1, M2, and M3) having hollow fired clay bricks of 30 × 20 × 15 cm size as shown in the Figure 2.17. M1 is the reference wall, M2 is the wall with MPCM and M3 is the wall having 10 mm of XPS insulation and MPCM. The size of the MPCM container is 30 × 17 × 2.8 cm and is made up of metal steel which is filled with paraffin wax RT18®. It was found that M2 and M3 have registered a reduction of 50% and 80% in thermal amplitude in comparison with M1. Additionally, a time delay of three hours in attaining peak temperature was achieved by M2 and M3. The thermal insulation provided in M3 affects the operation of the PCM.

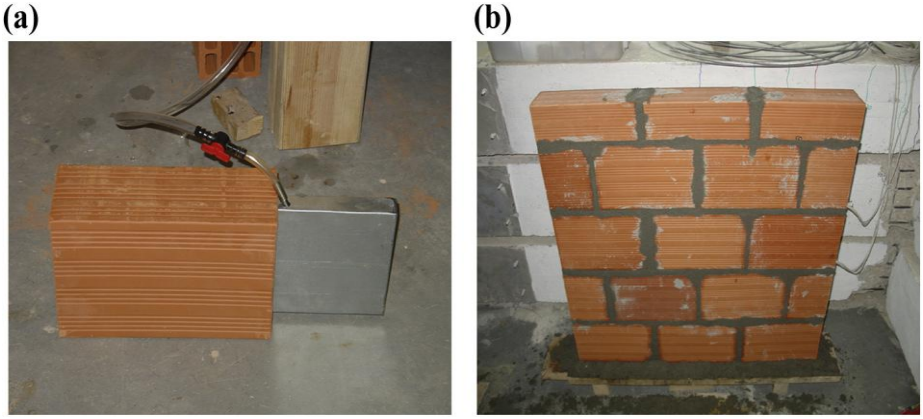

Figure 2.17 Hollow bricks with MPCM (100)

Figure 2.18 Bricks with PCM macrocapsules (101)

To evaluate the effect, of incorporating macrocapsules of PCM in the brick used for construction, on indoor thermal behavior, the (101) has tested the developed PCM bricks in the climatic chamber. Two wall specimens were prepared, one is having MPCM bricks as shown in the Figure 2.18, and the other one is prepared without PCM bricks. Steel is used as encapsulating material and RT18 was used as PCM. The results shows a reduction of 5 ˚C to 10 ˚C in thermal amplitude and a time delay of almost 3 hours in the wall specimen prepared using MPCM.

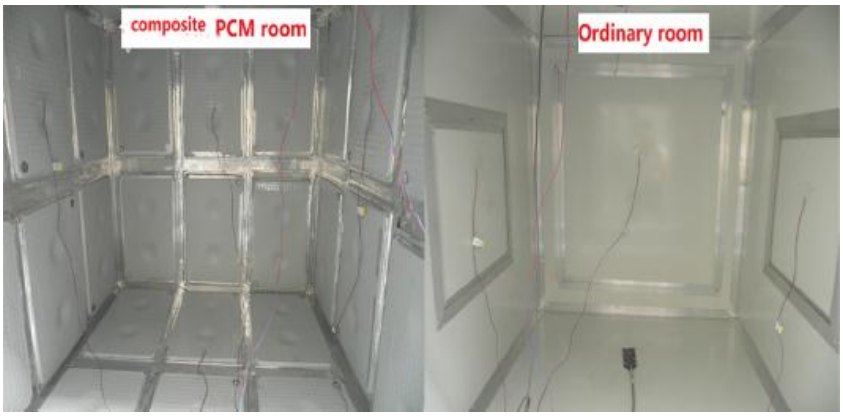

Figure 2.19 Inside view of composite PCM room and ordinary room (102)

The (102) has developed two rooms (1000 mm × 1000 mm × 1000 mm), one with macroencapsulated composite PCM, called composite PCM room and the other without

macroencapsulation, called ordinary room as shown in Figure 2.19. Two kinds of PCM, namely SP29 and RT18 from Rubitherm, were encapsulated in aluminum panels. SP29 was placed on the floor, ceiling and west wall while RT18 was placed on the south and the north wall of the composite PCM room. Both the room were placed and tested on the real outdoor environmental condition. Following are the findings from the experiment:

(a) In comparison to the ordinary room, the PCM room attains a temperature drop of 4.28 ˚C to 7.7 ˚C during the summer day and a temperature rise of 2.02 ˚C to 2.71 ˚C during the summer night. For winters, PCM room registered a temperature drop of 11.21 ˚C to 14.12 ˚C for a winter day and a temperature rise of 6.93 ˚C to 9.48 ˚C for a winter night.

(b) A reduction of 17.7% to 25.4 % in temperature fluctuation was recorded during winter and 28.8 % to 67.8 % during summer.

Three test rooms, in China, were developed by using perforated bricks (240 mm × 115 mm × 90 mm) and MPCM by (103) to evaluate the effect of free cooling, open window and door at night and forced ventilation at night. One test room is developed without PCM, the second test room is developed by incorporating macroencapsulated capric acid on the outside surface and third test room is developed by incorporating macroencapsulated 1-dodecanol on the inside surface. The material used for encapsulation is an aluminum panel of size 10 cm × 10 cm and having a thickness of 0.1 cm. Figure 2.20 (a) shows the aluminum panel used for encapsulation of the PCM and fig. 27 (b) shows the perforated brick and the test room site.

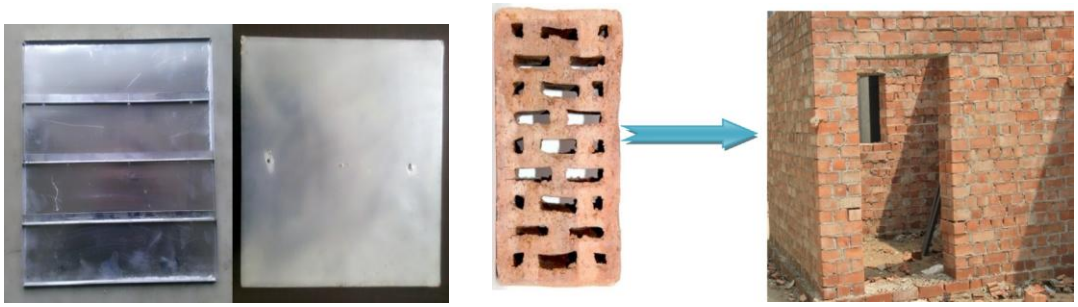

(a) (b)

Figure 2.20 (a) Encapsulation used for PCM (b) Test room and perforated brick (103)

The roof of all the test rooms was insulated using glass fiber reinforced cement board with a waterproofing layer. For night ventilation a window (800 mm × 500 mm) and a door (1800 mm × 800 mm) were also provided in all the test rooms. The results revealed that the maximum reduction in peak temperature was achieved by the test room having PCM on the inside surface. The MPCM also improves the time delay by 2.1 hours and 3 hours for outside surface PCM test room and inside surface PCM test room respectively. Figure 2.21 (a), (b) and (c) shows the variation in indoor and outdoor temperature for free cooling, open window and door at night and forced ventilation at night respectively. Reduction in thermal amplitude was also noticed in the test rooms having MPCM.

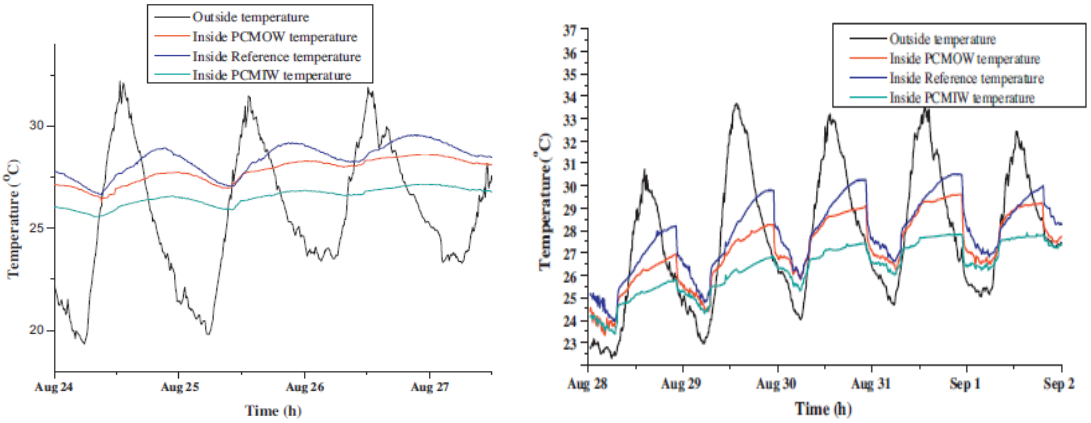

(a) (b)

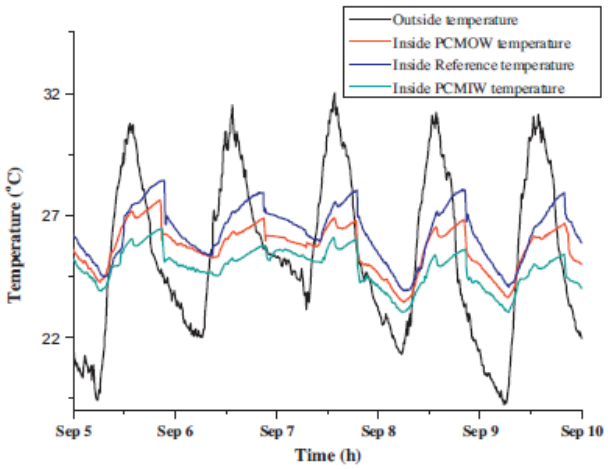

(c)

Figure 2.21 (a) Outdoor and indoor temperature in free cooling (b) Outdoor and indoor temperature during open window and door at night (c) Outdoor and indoor temperature during forced ventilation at night (103)

A study (104) proposed integration of macroPCM into polyvinyl acetate (PVA) to fabricate the wall tile. Figure 2.22 (a) shows the location of the macroPCM wall tile and fig. 29 (b) is the design model of the macroPCM tile. The PCM used for encapsulation is octadecane.

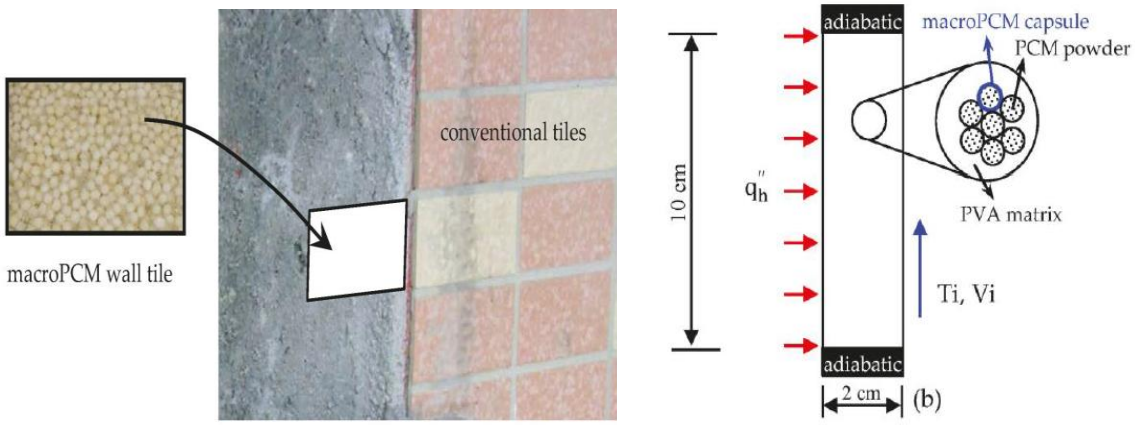

(a) (b)

Figure 2.22 (a) Location of macroPCM wall tile (b) Physical model of macroPCM wall tile (Not to scale) (104)

The results suggest that wall tile, made of PVA-macroPCM, has adequate thermal resistance and latent heat capacity to effectively regulate the indoor temperature. The tile produces low

indoor thermal flux as compared with other building materials. Additionally, with respect to strength and appearance the tiles are suitable to be used as indoor building material.

The relative location of the MPCM in the building envelope significantly affects the indoor thermal behavior of the building. Lots of studies are available which analyzed the performance of the PCM panels at different location and with varied PCM thickness incorporated in the building envelope. Two test houses of dimensions 1.83 m × 1.83 m × 1.22 m, as shown in Figure 2.23 (b), were developed by (105). One test house is without PCM called control house, while the other one is having MPCM (packed in aluminum foil sheets) in the south and the west wall. The thickness of the PCM sheet is 0.2 cm, width is 60.2 cm and the length is 40.6 cm, as shown in Figure 2.23 (a). The PCM used was hydrated salt having a melting point of 31.4 °C.

(a) (b)

Figure 2.23 (a) PCM packed in aluminum foil sheet (b) Test houses developed for study (105)

The PCM sheet was installed in the cavities of an insulated board in the south and west wall and was tested for a suitable location, according to the heat flux reduction, in the wall. The

optimum location of the PCM sheet was in the 3rd and in the 2nd cavity, from inside, in the south and the west wall respectively. These locations recorded a 51.3% and 29.7% reduction in heat flux in the south and the west wall respectively. The peak heat flux time delays was 6.3 hours when PCM sheet was placed in the 1st cavity of the south wall and 2.3 hours when PCM sheet was placed in the 2nd cavity of the west wall.

A paraffin-based PCM called n-octadecane was used by (106) as PCM to be macroencapsulated in the copper pipes which are then placed inside the wall. Two sets of pipes were used having a diameter of 1.27 cm and 1.9 cm as shown in the Figure 2.24. The small-sized pipes were placed at 5.08 cm apart and large sized pipes were placed at 9.4 cm apart as shown in the Figure 2.24. For testing, a dynamic wall simulator was used in which two types of configuration of the MPCM were used. The first is "middle depth" (MD) configuration in which PCM pipes were placed in the middle of the wall and the other configuration is "next to wallboard" (NTW) in which PCM was placed next to the wallboard. Two layers of fiberglass batt insulation having a resistance value of 1.94 $W/m^2/°C$ were also placed over and beneath the pipes. The results depict that, in middle depth configuration the maximum energy savings of 63.81 $W\text{-}hr/m^2$ and a highest time delay of about 116 minutes were observed for pipe diameter of 1.27 cm. In next to wallboard configuration, the maximum energy saving of 32.67 $W\text{-}hr/m^2$ was observed for 1.9 cm of diameter pipes. It is also noticed that in this configuration, the heat storage capability of the PCM could not be fully used because of the low temperature around the pipe. For effective heat flux reduction and energy savings, middle depth configuration with a smaller pipe diameter must be used.

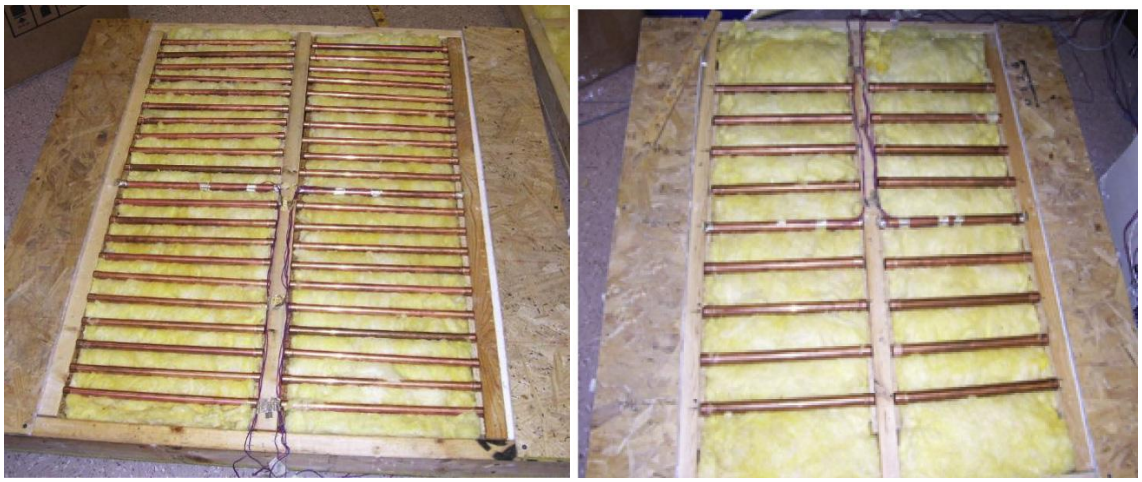

Figure 2.24 Wall assembly used for experimentation in the dynamic wall simulator (106)

Two identical test rooms (3 m × 2.5 m × 2 m) were developed by (107) to evaluate the energy savings and thermal comfort. One room is having PCM, encapsulated in an aluminum container, on the roof and the wall while the other room is developed without using PCM. The PCM used is a mixture of 40% oil and 60% paraffin wax. Figure 2.25 (a) and Figure 2.25 (b) shows the experimental setup and the encapsulated PCM in the aluminum panel.

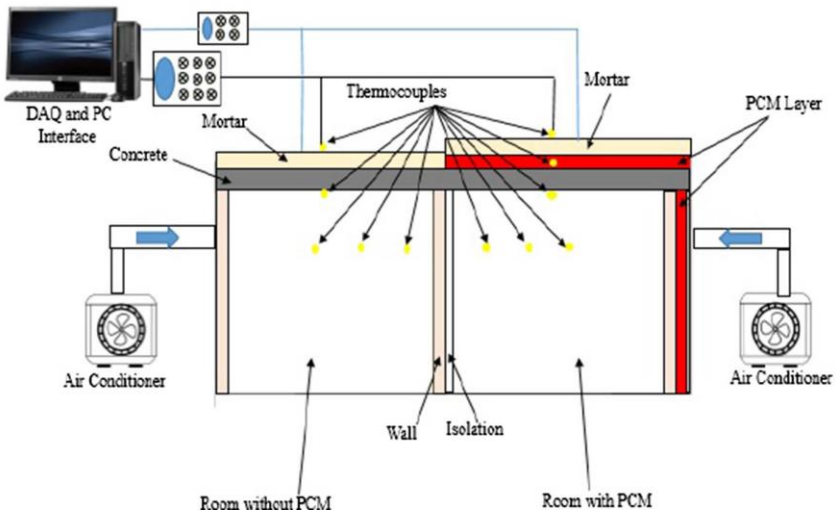

(a)

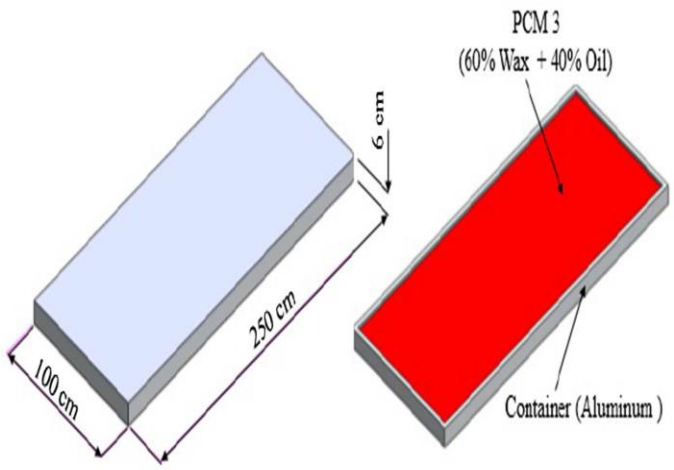

(b)

Figure 2.25 (a) Experimental setup of the developed test rooms integrated with PCM in aluminum containers (b) Encapsulated PCM in aluminum containers (107)

common building material is used to develop both the test room, i.e. bottom slab is made of 12 cm concrete, top slab is made of 10 cm mortar and brick mixture and the walls are made of cement, common brick and gypsum. Varying thickness (2.5 cm, 4 cm, and 6 cm) of PCM is used in the roof of PCM room, while the walls are having a 2.5 cm thick layer of encapsulated PCM. The test results revealed that there is a reduction in heat flux penetration ratio of 38.45%, 59.25% and 74.75% of 6 cm, 4 cm and 2.5 cm thick PCM layer, respectively. A reduction of 45% in energy has been achieved in maintaining the indoor temperature of 24 °C in the PCM room in comparison to the room without PCM.

Reduction in cooling load, by encapsulating the PCM in aluminum container and integrating it with the internal wall of the building envelope, was evaluated by (108). Two identical test rooms (1.5 m × 1.5 m × 1 m) were developed, one without PCM called reference room and the other with PCM called the experimental room. Paraffin wax, with a melting temperature of 44 °C, was used as PCM and was filled in the aluminum container as shown in the Figure 2.26.

Figure 2.26 Test room with PCM encapsulation (108)

The investigation was done by varying the thickness of the PCM i.e. 1 cm and 2 cm and comparing their results with reference test room. The results show electricity cost saving of 1.35 Dollar/day/m^3 in cooling load with 1cm thickness of the PCM wall, 0.88 Dollar/Day/m^3 with 1 cm thickness of PCM for ceiling, 1.19 Dollar/Day m^3 with 2cm thickness of PCM for south wall, 1.21 Dollar/Day/m^3 with 2cm thickness of PCM for west wall, 1.08 Dollar/Day/m^3 with 2cm thickness of PCM for north wall, 0.58 Dollar/Day m^3 with 2 cm thickness of PCM for east wall.

2.2.2 MPCM incorporated in Air Handling Unit

Various thermal energy storage systems and air handling units, using MPCM, are developed and analyzed by the researchers to identify the effectiveness of the PCM in regulating the indoor thermal behavior of the building. An innovative thermal energy storage system which consists of prefabricated concrete slab integrated with MPCM was developed and tested by (109) to analyze the charging and discharging of the PCM during heating and cooling mode. The schematic diagram of the setup was shown in Figure 2.27.

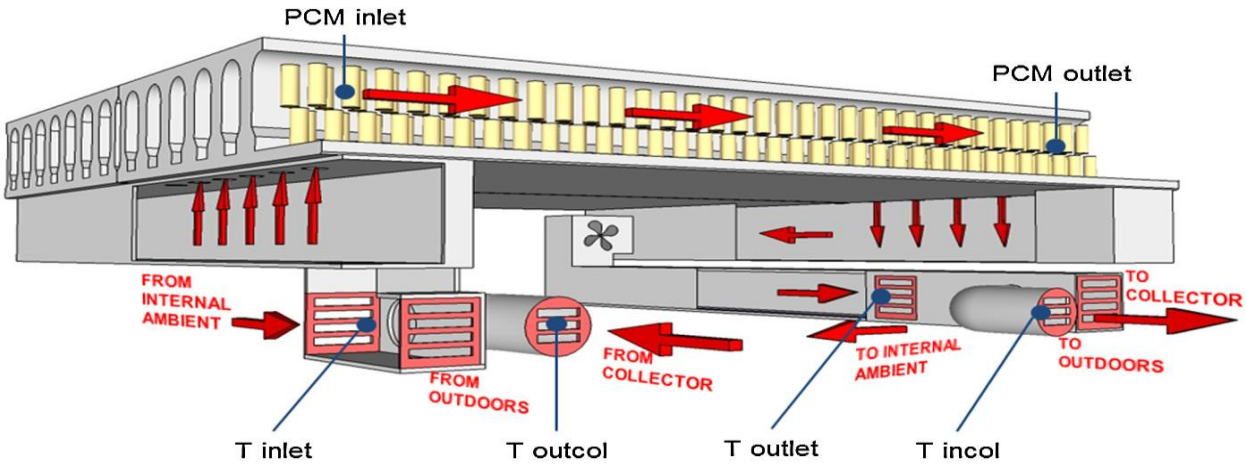

Figure 2.27 Schematic of the concrete slab (109)

The concrete slab has a thickness of 30 cm, with a surface area of 2.4 m × 2.4 m and having 14 channels where MPCM has placed. The presence of holes in the channel ensures the airflow using a duct and a fan. A solar air collector (1.3 m^2) was also installed in the prototype to ensure heat supply during winter mode. The PCM used is RT21 and was encapsulated in aluminum tubes of 12 mm diameter and 100 mm height. Around 52 kg of PCM was encapsulated in 1456 tubes. All these tubes are then inserted inside the channels. The results suggest that, in summer mode, the active slab is able to almost charge 100% of the PCM for 70% of the summer days. Whereas, in winters the solar air collector with an efficiency of 30% is sufficient to completely charge the PCM throughout the winter season. In winter mode, 70% of charged and discharged efficiency was registered. In both winter and summer mode energy losses were registered during charging and discharging of the PCM, which can attribute to the energy gain (heating and cooling) in the buildings.

An experimental investigation for free cooling of building in hot-arid climatic condition using paraffin RT28HC as MPCM has been carried out by (110). The developed thermal energy storage system consists of 16 MPCM modules stacked horizontally over each other in eight parallel rows with two modules in each row as shown in Figure 2.28. The

authors have analyzed the effect of compactness of modules in the thermal system by varying the height of the air passages between the PCM modules. The air passage gaps considered in this study are 10 mm, 15 mm, and 20 mm. The whole thermal energy storage unit was surrounded by 50 mm thick polyisocyanurate foam of 0.022 W/mk thermal conductivity.

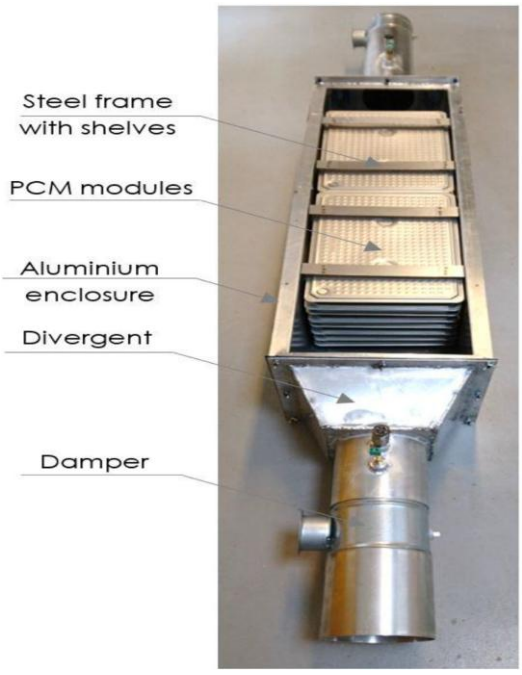

Figure 2.28 Thermal energy storage unit developed by using MPCM for free cooling (110)

The findings reveal that the air flow rate greatly affects the charging of the PCM. Higher flow rates are required to accelerate the solidification whereas, lower flow rates are recommended to maintain prolong thermal comfort. However, thermal comfort remains unaffected by varying the size of the air gap. Consequently, a compact design of the thermal energy system with narrow passages is suitable for free cooling in buildings.

A commercially available paraffin based PCM named ZDJN28 with melting temperature of 28 °C was encapsulated in HDPE (high-density polyethylene) slabs and was

tested for thermal response in a wind tunnel experimental setup, as shown in the Figure 2.29, developed by (111). The findings were based on the effect of air temperature, air velocity, and HDPE slab inclination. The outside dimensions of the slab are 315 mm × 28 mm × 200 mm (L×W×H) and having a thickness of 1 mm.

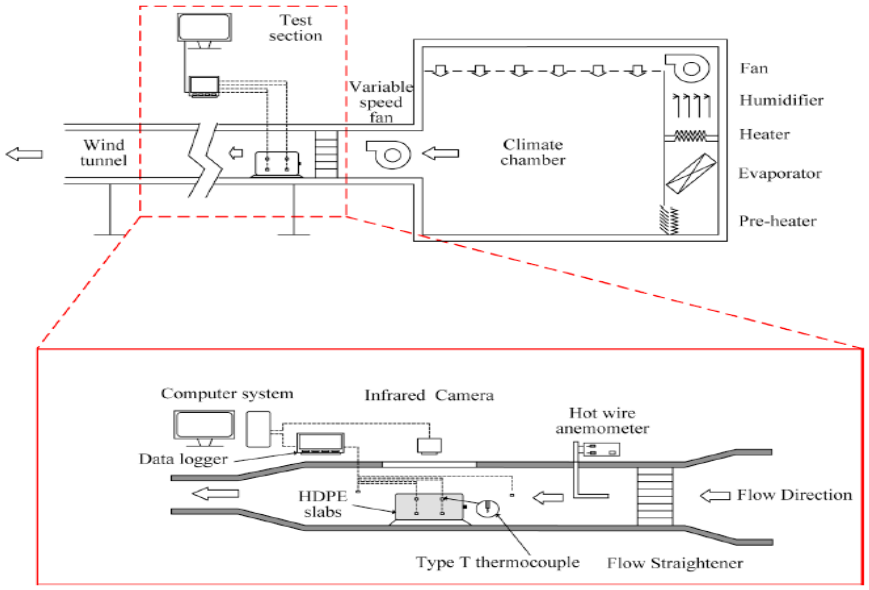

Figure 2.29 Schematic of the experimental setup (111)

It was analyzed that the increase in the air velocity from 1 m/s to 5 m/s will reduce the melting time of MPCM from 36.6% to 46.7%. There is no significant rise in the stored heat in all the three cases, i.e. as a function of air velocity, air temperature, and slab inclination. A maximum of 20.2 % rise in the stored heat was observed when the air temperature was set at 55 °C. Increasing the inclination angle of the slab will increase the energy charging speed.

An air-PCM heat exchanger for peak load management in the buildings was developed and tested by (112) using MPCM. 16 Aluminum plates were used to macroencapsulate the 37D PCM (from Microtek) as shown in the Figure 2.30. The heat exchanger is 1.05 m long, 0.75 m wide and 0.25 m high with a carrying capacity of 31.8 kg

of PCM. This heat exchanger is coupled with an experimental test cell called hybcell (5.1 m long, 3.5 m wide, and 2.9 m high). The results suggest that the heat exchanger is capable of maintaining the indoor thermal comfort at a temperature of 21 °C for almost two hours and also able to reduce the peak demand.

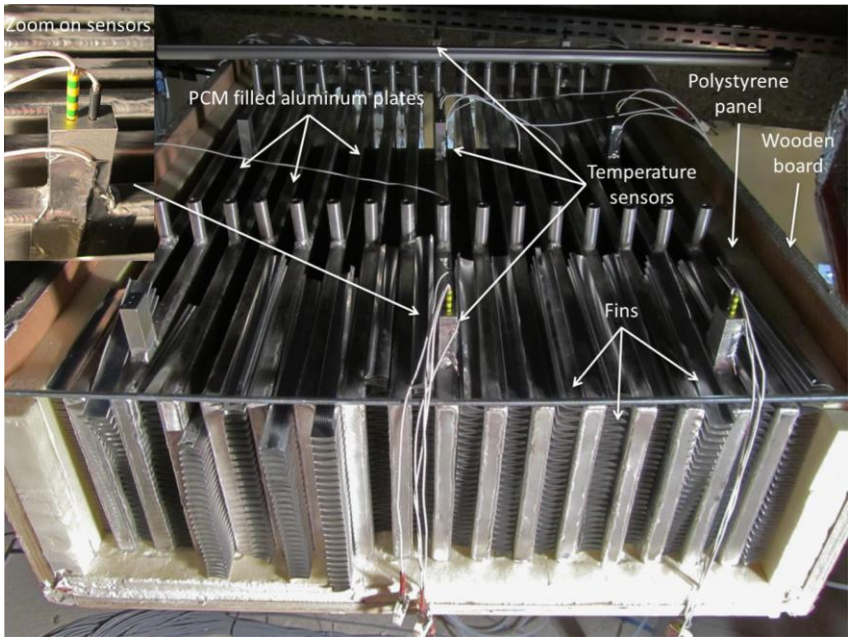

Figure 2.30 Air-PCM heat exchanger having MPCM (112)

An experimental facility, to evaluate the thermal performance of two types of paraffinic PCM and a salt hydrate PCM, was developed by (113). A heat exchanger was developed, as shown in the Figure 2.31, using three types of MPCM RT25, RT27 and SP24E. All these PCM are encapsulated in aluminum panel, which are purchased from Rubitherm, as shown in Figure 2.32. The effect of air mass flow rate and inlet air temperature on the cooling behavior of the MPCM was studied. The results revealed that all the three PCM are capable of providing free cooling to the building under the South African climate condition. The salt hydrate PCM panel has the highest energy absorption capacity.

The paraffinic PCM shows high instantaneous heat absorption with short heat absorption duration while salt hydrate exhibits sort instantaneous heat absorption with high heat absorption duration.

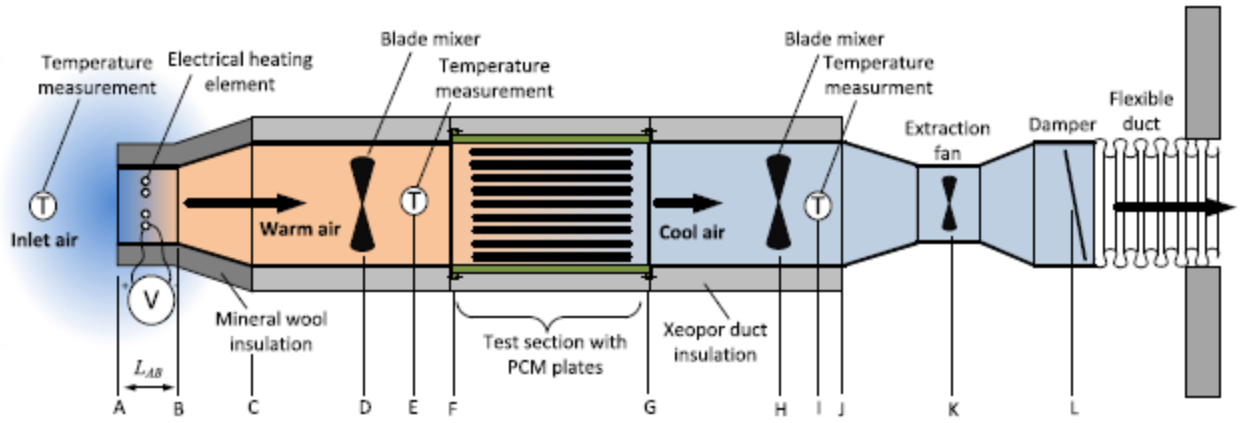

Figure 2.31 Schematic of heat exchanger having MPCM (113)

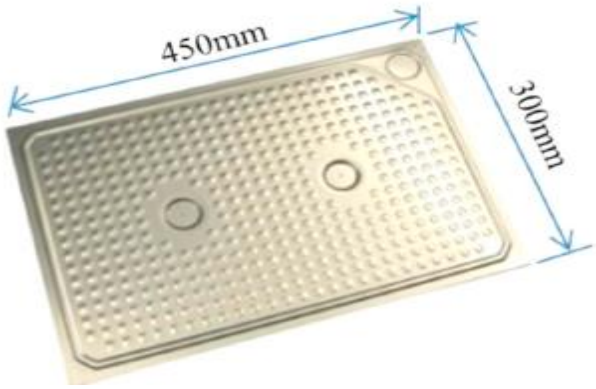

Figure 2.32 Commercially available MPCM panel (113)

2.2.3 Performance enhancement of macroencapsulated PCM

MPCM often faces shortcomings like poor thermal conductivity and interfacial bonding with the matrix material, which reduces the thermal function of the PCM. However, these demerits will be overcome by selecting a suitable type of container/shell which will

enhance the heat transfer rate and improves the thermal stability of the PCM. The (114) have used a metal clamp, as shown in the Figure 2.33, to improve both bonding and thermal conductivity of the MPCM with matrix material. The PCM (Octadecane) was macroencapsulated in HSB (Hollow steel ball) of 22 mm diameter. Figure 2.34 shows the prepared HSB and the metal clamp. Various samples of HSB concrete ranging from 25%, 50%, 75% and 100% volume replacement of coarse aggregate with and without metal clamp were prepared. The concrete panel was prepared using ordinary Portland cement, fine aggregate, coarse aggregate and river sand. The results suggest that there is less reduction in compressive strength of the samples with the metal clamp in comparison to samples without the metal clamp. There is an increase of 14% and 22% in the strength of 50% HSBC and 70% HSBC samples with clamp respectively. The HSBC sample with clamp reduces the indoor temperature fluctuations and also reduces the indoor cooling and heating load significantly. These HSB with MPCM have great potential of thermal energy storage in the building envelope.

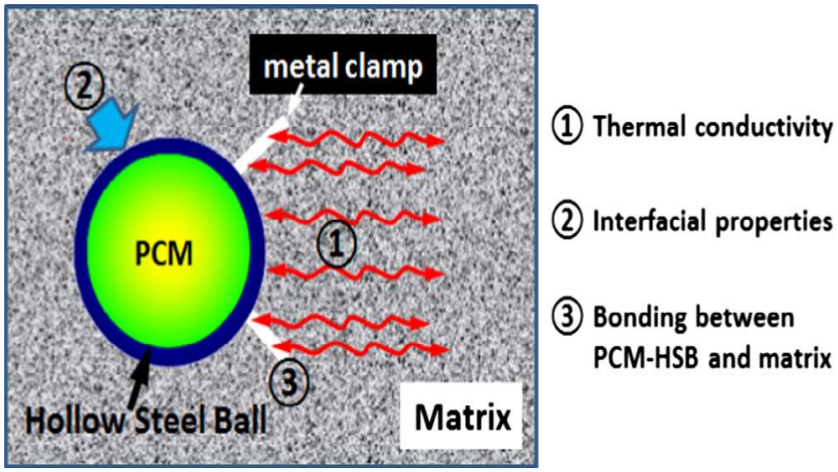

Figure 2.33 Layout of Hollow Steel Ball (HSB) with metal clamp (114)

Figure 2.34 HSB without metal clamp, metal clamp and HSB with metal clamp (From top to bottom) (114)

The (115) have developed a MPCM hollow steel ball (PCM-HSB), as shown in Figure 2.35, using octadecane as PCM and has tested for mechanical and thermal behavior, when integrated with concrete. Various samples of the concrete panel, as per the specifications given in Table 2.4, was prepared and investigated. It was found that the MPCM-HSB has the potential to reduce the peak indoor temperature and minimize the temperature fluctuations. Each PCM-HSB ball carries upto 80.3% PCM by mass and also the leakage, after 1600 thermal cycles, was reduced to less than 1%. This shows that the PCM-HSB has high reliability with long term stability to be used in buildings. Additionally, the strength of SC-100% was found to be 22 MPA, which is suitable to use in construction material.

(a) (b)

Figure 2.35 (a) PCM-HSB ball secured with rivet and epoxy (b) Cut section of HSB (115)

Table 2.4 Composition of prepared concrete panel samples (115)

Type	Cement (kg)	Water (kg)	Sand (kg)	Gravel (kg)	PCM-HSB (kg)
NC	400	140	787	1092	0
SC-25%	400	140	787	819	175
SC-50%	400	140	787	546	351
SC-75%	400	140	787	273	526
SC-100%	400	140	787	0	701

The (116) have analyzed different shapes of MPCM, integrated into the concrete blocks, to investigate the effect on heat transfer during crystallization and melting of PCM. The eutectic mixture of $MgCl_2.6H_2O$ and $CaCl_2.6H_2O$ was used as PCM and aluminum compound foil was used to prepare various shapes of encapsulation. Ten sample blocks, including reference block, was prepared which includes two blocks of MPCM in a cuboid shape, two in the cylindrical shape, four in the plate shape and one in a spherical shape. All the prepared samples are shown in Figure 2.36. All these samples are then tested in an experimental setup made up of a wooden frame which consists of infrared radiator and a cooler.

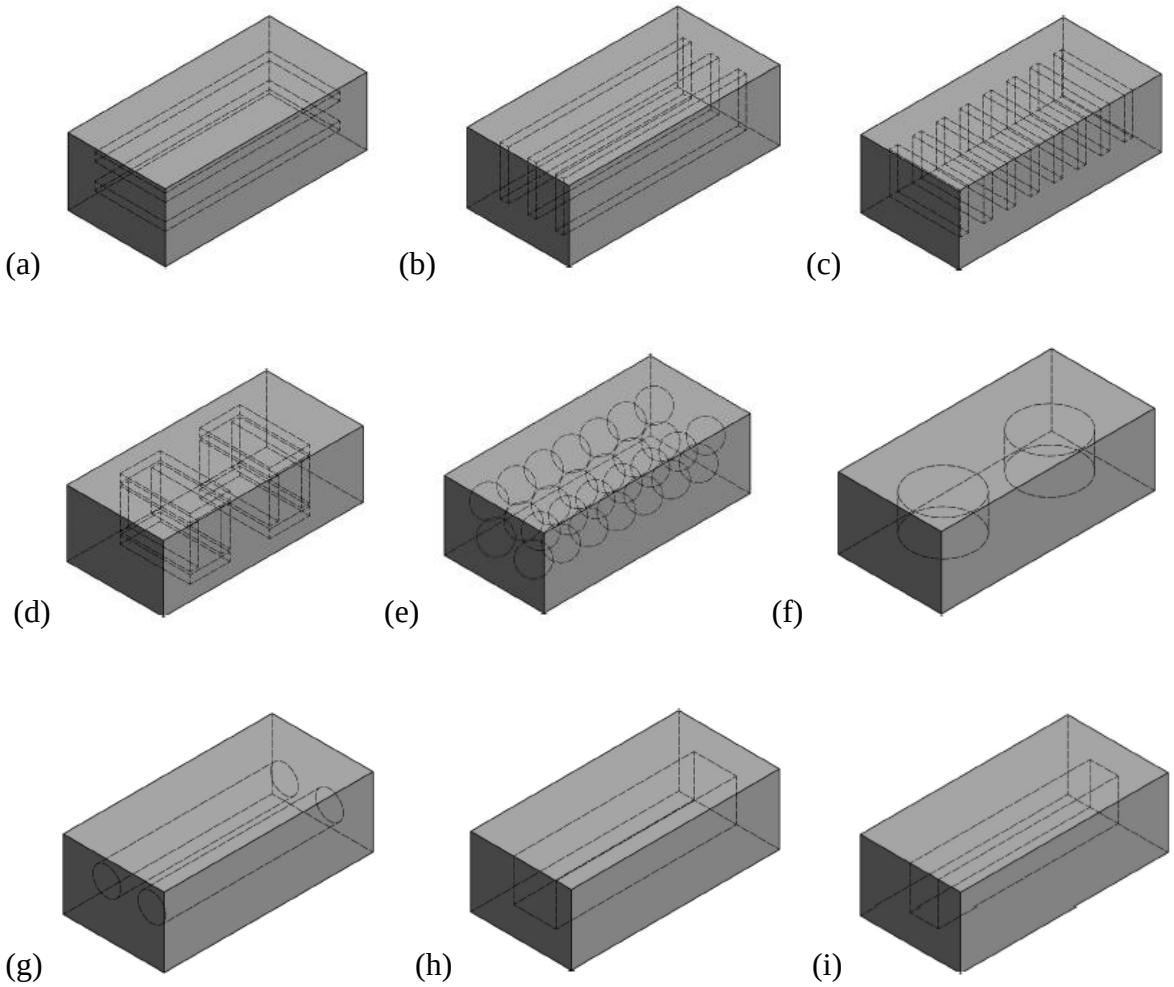

Figure 2.36 Samples of concrete block prepared by using various shapes of encapsulation (a) Superimposed elongated plates 1 design (b) Adjacent setup elongated plates 2 design (c) Separated plates 3 design (d) Complex plate 4 design (e) Spherical shape (f) Cylinder 1 design (g) Cylinder 2 design (h) Cuboid 1 with 1 kg pcm (i) Cuboid 2 with 1.5 kg pcm (116)

The study finds that sphere shape encapsulated PCM shows fastest melting because of the large heat transfer surface and uneven distribution as shown in the Figure 2.37 (a). Whereas, cuboid block having 1.5 kg PCM has shown the slowest melting speed, among all the samples, because of higher PCM mass. Also, the crystallization with this shape requires more time in comparison to other shapes as shown in the Figure 2.38 (b).

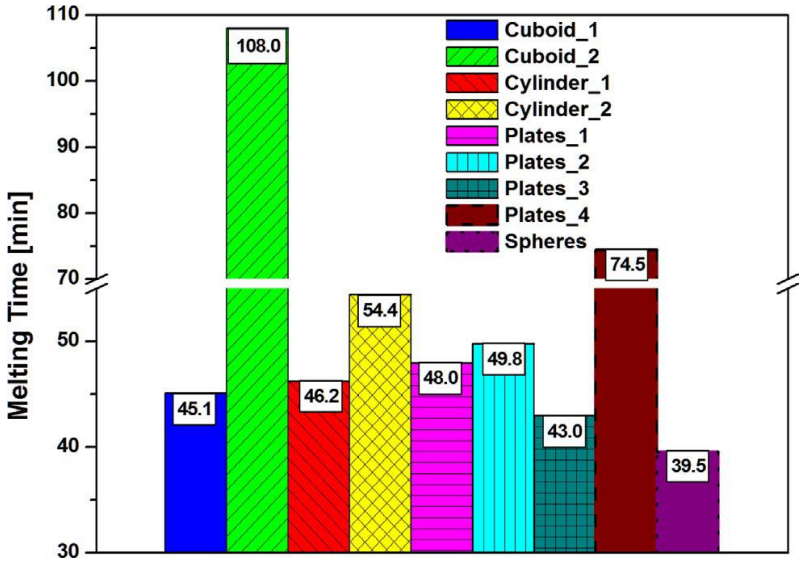

(a)

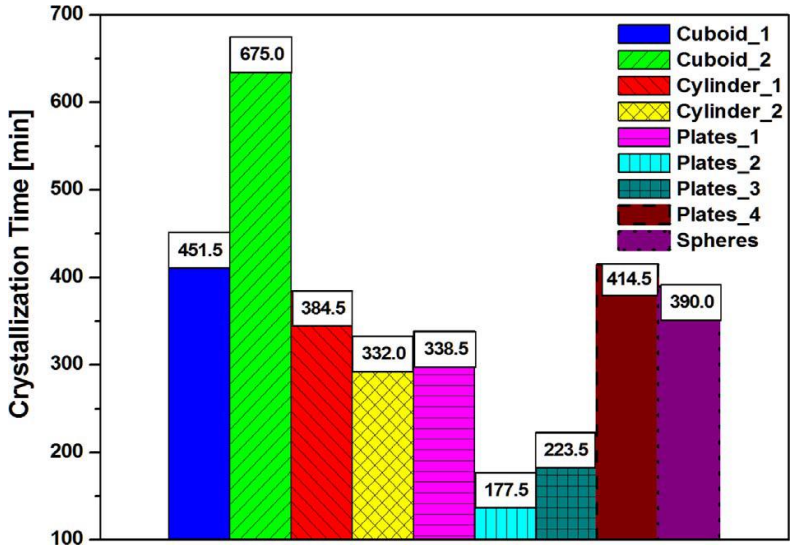

(b)

Figure 2.37 (a) Melting time (b) Crystallization time of various prepared concrete block samples (116)

Cylindrical shape PCM shows a slow melting rate because of the lower position of the upper face and lesser heat transfer surface area, pointing towards the heat source. Plate-shaped encapsulated PCM shows different thermal response to the heating source depending upon the position, shape, size, and orientation inside the concrete block.

2.2.4 Compatibility with shell/container material

To enhance the thermal performance of the PCM the compatibility of the encapsulated PCM with the shell/container material is important. High compatibility not only enhances the thermal performance of the MPCM but also increases the long term reliability and stability of the PCM. The (117) have shown a comparative analysis of various paraffin PCM on the chemical compatibility with 17 different metallic and plastic containers used for encapsulation of the PCM. Since, chemical compatibility such as corrosion, wear, fire resistant and etc. are important for long term stability and reliability of the material used as a container for encapsulation.

Table 2.5 Comparative analysis chart on chemical compatibility of PCM with container material for encapsulation (117)

Material	Nonadocane	Eicosane	Docasane	PW48	PW52	PW58
6061 Aluminum	✓	✓	✓	✓	✓	✓
6063 Aluminum	✓	✓	✓	✓	✓	✓
5052 Aluminum	✓	✓	✓	✓	✓	✓
304 Stainless steel	✓	✓	✓	✓	✓	✓
316 Stainless steel	✓	✓	✓	✓	✓	✓
101 Copper	✓	!	!	✓	✓	✓
110 Copper	✓	✓	✓	✓	✓	✓
Ni C7521	✓	✓	✓	✓	✓	✓
Mg AZ 51D	✓	✓	✓	✓	!	!
Polycarbonate film	✓	✓	✓	✓	✓	✓
Polypropylene	×	×	×	×	×	×
Cast Acrylic	!	!	!	!	!	✓
Type 1 PVC	✓	✓	✓	✓	✓	✓
Silicon Rubber	×	×	×	×	×	×
ABS plastic	!	✓	✓	✓	!	✓
Nylon	!	×	×	!	!	!

✓ = Recommended for long term use ($C_R < 10$ mg cm^{-2} yr^{-1})

! = Caution recommended ($10 \leq C_R \leq 50$ mg cm^{-2} yr^{-1})

× = Not recommended for use ($C_R \geq 50$ mg cm^{-2} yr^{-1})

The chemical compatibility was determined from the corrosion rate value (C_r), calculated after 1, 2 and 6 weeks of immersion in the liquid PCM at a temperature of 75 ˚C. The

material is suitable for encapsulation of PCM only if, the degradation rate due to corrosion is less than 10 mg/cm^2/year. A compatibility chart, of various metals with different PCM, is shown in Table 2.5. The thermal cycle (~3000) test also reveals that the selected PCM are having long term stability of almost 8 years in solar thermal systems.

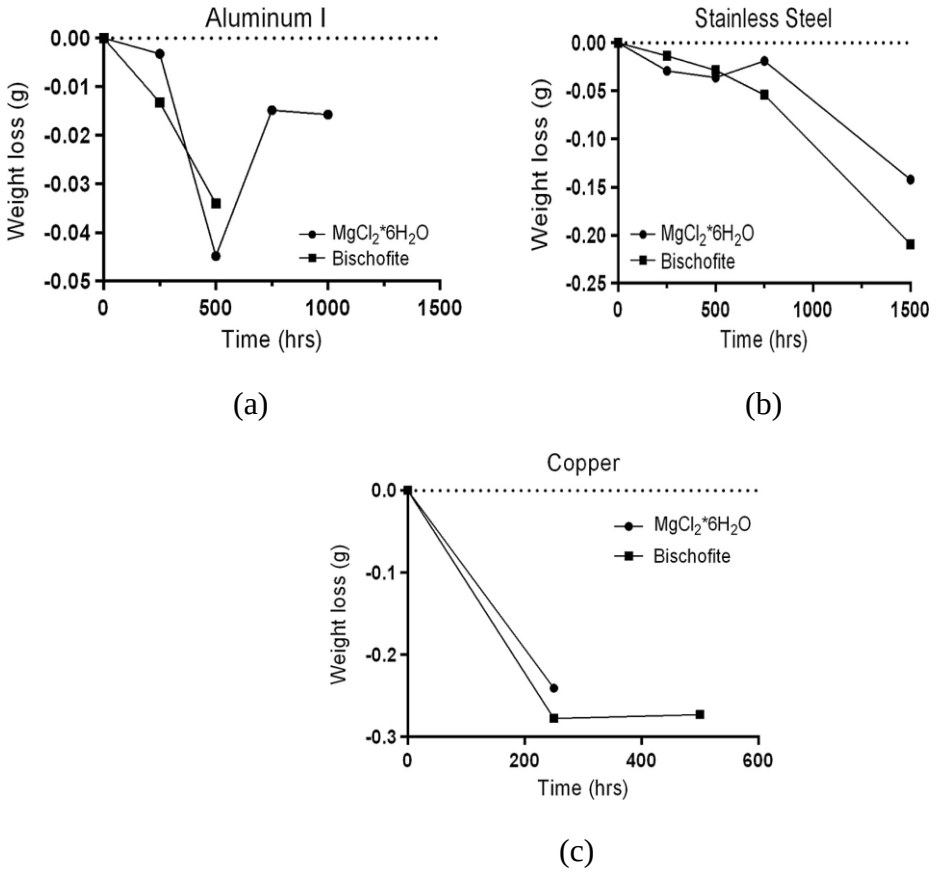

Figure 2.38 Weight loss of (a) Aluminum (b) Stainless steel (c) Copper in inorganic PCM (118)

The compatibility of metal sheets of copper, aluminum and stainless steel for macroencapsulation of inorganic phase change material was studied by (118). The behavior of $MgCl_2.6H_2O$ with Bischofite was compared on the basis of deterioration due to corrosion. The metals were partially immersed in the molten salt hydrates at a temperature of 120 ˚C for the period of 1500 hours. Figure 2.38 represents the deterioration of copper, stainless steel, and aluminum due to corrosion. The study shows that minimum corrosion had

occurred on all the immersed surfaces of metals while a severe presence of corrosion had been identified at the salt-air interface. It is suggested that care should be taken to avoid the presence of air while designing the thermal energy system using these metals for macroencapsulation. The (119) have evaluated the effect of corrosion on copper, aluminum, stainless steel 316, and carbon steel when used as an encapsulating container for PCM. The test was conducted for both heating and cooling mode. A set of eleven PCM, five PCM are having a melting temperature of around 10 °C and six PCM are having a melting temperature of around 46 °C, was used. PCM having a low melting temperature are analyzed for cooling application and PCM having a high melting temperature are studied for heating application. Corrosion rate was analyzed by dipping the metal sheets for a period of 1 week, 4 weeks and 12 weeks. Table 2.6 and table 2.7 show the deterioration rate of the metals due to corrosion. The metal-PCM combination with a low rate of corrosion rate is suitable to be used as MPCM in buildings.

Table 2.6 Rate of corrosion ($mg/cm^2/yr$) of different metals and alloys with all combinations of PCM for cooling application (119)

	Copper			Stainless steel			Carbon steel			Aluminium		
PCM	1wk	4 wk	12 wk	1wk	4 wk	12 wk	1wk	4 wk	12 wk	1wk	4 wk	12 wk
S10	2.1	22.2	356.7	2.1	0.0	0.1	103.2	22.4	9.5	29.2	9.4	2.0
C10	1931.4	22.9	96	1.0	0.5	0.2	88.6	16.7	35.5	3.1	4.2	3.5
$ZnCl_2.3H_2O$	0.0	4.4	1.7	1.0	0.5	0.4	79.3	8.6	12.2	n.d.	878.6	7303
$NaOH.1.5H_2o$	119.9	14.9	21.6	1.0	0.0	0.3	27.1	11.7	5.7	n.d.	n.d.	n.d.
$K_2HPO_4.6H_2O$	7.3	19.6	3.3	3.1	0.0	1.0	131.4	42.2	17.6	108.5	84.5	106.7

n.d. stands for non available data

Table 2.7 Rate of corrosion (mg/cm^2/yr) of different metals and alloys with all combinations of PCM for heating application (119)

PCM	Copper			Stainless steel			Carbon steel			Aluminum		
	1wk	4 wk	12 wk	1wk	4 wk	12 wk	1wk	4 wk	12 wk	1wk	4 wk	12 wk
S46	843.7	407.5	323.7	0.0	-0.8	-0.3	89.7	83.7	27.4	27.1	0.0	2.0
C48	146.0	1613.0	14.9	0.0	0.0	-0.2	1.0	4.7	5.5	2.1	0.8	3.5
$MgSO_4.7H_2O$	121.0	43.4	21.0	0.0	0.0	-0.3	749.8	277.4	80.5	5.2.	4.4	7303
$Zn(NO_3)_2.4H_2o$	1167.0	644.0	338.5	0.0	0.0	-0.2	1741.6	484.4	196.2	181.5	206.2	162.2
$K_3PO_4.7H_2O$	145.0	6.5	11.5	0.0	0.0	0.1	0.0	0.8	3.7	n.d.	84.5	n.d.
$Na_2S_2O_3.5H_2O$	2663.5	437.0	339.5	0.0	0.0	0.3	41.7	15.6	4.5	40.7	84.5	5.6

n.d. stands for non available data

Different methods of macroencapsulation of 50 wt% $MgCl_2.6H_2O$ and 50 wt% $CaCl_2.6H_2O$ was investigated by (120). The results suggest that the foils with a layer of aluminum or polyvinylidene chloride and liquid spar varnish with additives are suitable material. Rubber material such as liquid EPDM, liquid rubber (Noxyde), extruded tape (RB81), malleable modeling clay (RB IX), and injectable mass (RB 2759) are also suitable.

2.3 Shape stabilized PCM

PCM suffers from the drawbacks of poor thermal conductivity and leakage during phase transition. To overcome these limitations, supporting materials are mixed with PCM. Supporting material is of two types, one is a porous material which prevents the leakage of the PCM and the other is nano-material which improves the thermal characteristics of the PCM. When the PCM gets loaded with these two supporting material then it is called as shape stabilized composite PCM (ss-CPCM) or shape stabilized PCM, as shown in Figure 2.39.

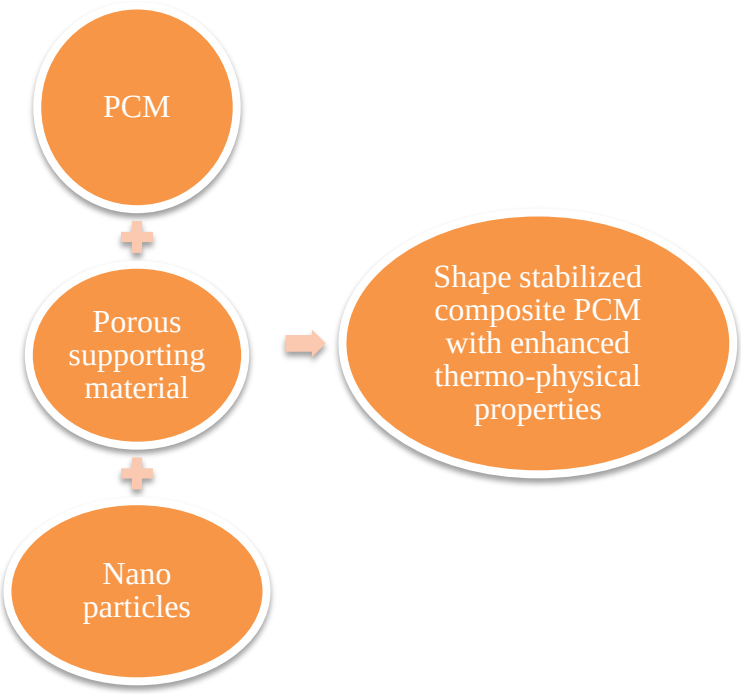

Figure 2.39 Scheme of preparation of shape stabilized composite PCM

Supporting material overcomes the limitation of poor thermal conductivity and leakage of the PCM. However, it must be noted that in most of the studies, the thermal energy storage capacity of the shape stabilized PCM reduced in comparison to original PCM sample. This is because of the non-participation of the supporting material molecules in thermal energy storage.

2.3.1 Porous material used for the improvement of thermo-physical properties

The porous material supports the PCM because of larger surface area, high thermal conductivity, and better chemical compatibility (121). The interaction of the PCM and the porous material occurs due to capillary force, Van Der Waals' force, surface tension, and hydrogen bond. This interaction restricts the leakage of the PCM within the porous material (122). Various types of porous materials are used and developed in recent times to improve the containment of the PCM. A broad classification of the porous material used as a supporting matrix for the development of shape stabilized PCM are shown in Table 2.8. The

loading of the PCM in the porous material is done by vacuum impregnation, ultrasonic oscillation and melting adsorption method.

Table 2.8 Classification and properties of porous supporting material for PCM (123)

Porous material				
Porous carbon	**Graphite schaffolds**	**Polyurethane foam**	**Silica schaffolds**	**Clays**
• Adjustable morphology • Low density • Excellent stability • Earth abundant source • Non-toxic • Excellent capillarity	• High thermal conductivity • Large pore volume • High thermal stability • Low density • Flame retardant	• Light weight • High strength/weigh t ratio • Excellent insulator • High energy absorbency • High flammability	• Highly porous • Excellent mechanical properties • Thermally and chemically stable • Abundant availability • Relatively high price	• Thermally stable • Low price • Compatible with building material • Naturally porous • Poor mechanical properties

2.3.2 Porous carbon

Porous carbons are made through pyrolysis and by activation of natural carbon as well as synthetic precursors. Porous carbons are generally derived from biomass and waste product and therefore they are cheaper, non-toxic, and widely available. Because of their superior properties, these are widely used as precursors for carbon-based porous materials in super-capacitor (124), fuel cells (125), lithium-ion batteries (126), and other fields. Carbon-based porous material has generated wide interest as supporting material for PCM because of low density, flexible morphology, excellent thermal stability, and high electronic conductivity (127). The (128) has developed shape stabilized composite PCM supported with eggplant-derived porous carbon and loaded with PEG to improve solar-to-thermal energy conversion

through the vacuum impregnation method. It is three dimensional spongy like biological porous carbon derived from the eggplant. They found that the biological porous carbon consists of nanopores and macropores having an average diameter of about 44.758 µm and a high PEG loading of 90.1 wt%. The enthalpy of the shape stabilized PCM is 149 J/g. The developed shape stabilized PCM also shows good thermal stability and enhanced thermal conductivity. The (129) has prepared porous carbon from dewaxed cotton having 90-95% cellulose using $Mg(OH)_2$ to develop shape stabilized PCM. This porous carbon has a high surface area with interconnected pores. The prepared shape stabilized PCM has high encapsulation, enthalpy, and better reliability. The encapsulation capacity of the porous carbon obtained at 700 °C, 800 °C and 900 °C is 85%, 90%, and 88% with an enthalpy of 204.4 kJ/kg, 219.4 kJ/kg, and 215.5 kJ/kg respectively. The (130) has prepared porous carbon from fresh potatoes and was used as supporting material for PEG to develop shape stabilized composite PCM (ss-CPCM).

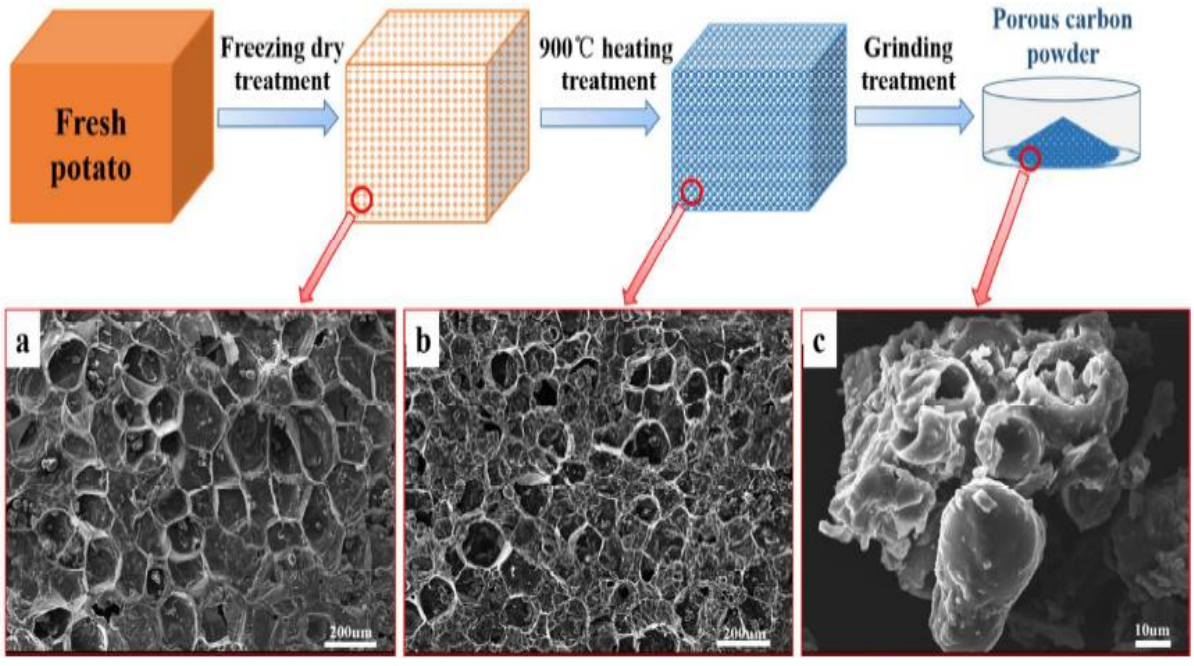

Figure 2.40 Scheme of preparation of porous carbon supporting material from fresh potato (130)

The porous carbon from fresh potatoes was prepared through deep freezing and heat treatment as shown in the Figure 2.40. The developed porous carbon has an average pore diameter of 204.7 nm, porosity of 73.4 and, surface area of 42.6 m^2/g. The PEG was then incorporated into the pores of porous carbon through ultrasonication. The developed shape stabilized PCM (PEG/Porous carbon ratio of 1:1) has a melting enthalpy of 91.80 J/g. This study also revealed excellent thermal stability and good shape stability of the shape stabilized PCM. The (131) has prepared carbon aerogel from the leaves of the succulent plant to support paraffin and to develop shape stabilized PCM as shown in Figure 2.41. The succulent based carbon aerogel consists of epidermis tissue, palisade tissue, and spongy tissue. Spongy tissue is the major component of leave, consist of spherical cells of size 200 to 250 micrometers. Epidermis and palisade act to prevent the leakage of the paraffin wax. The shape stabilized PCM achieved 95 wt% loading of the PCM along with the latent heat of 133.1 J/g and thermal conductivity of 0.427 W/mK. The study also suggests excellent thermal stability and leakage proof characteristics of the shape stabilized PCM.

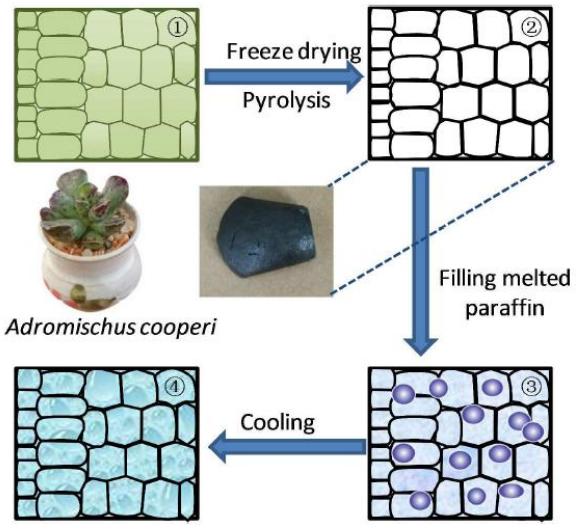

Figure 2.41 Scheme of preparation of succulent based carbon aerogel (131)

The (132) has used mesoporous N-doped porous carbon to prepare shape stabilized PCM by impregnating the eutectic mixture of myristic-stearic acid. The porous carbon was prepared from the reaction of melamine and glucose in the presence of KCL/$ZnCl_2$ as shown in Figure 2.42. The composite has achieved a maximum loading of 88% along with high stability after 100 thermal cycles. The heat storage capacity was 164.33 kJ/kg and enhancement of 117.65% in thermal conductivity was noted.

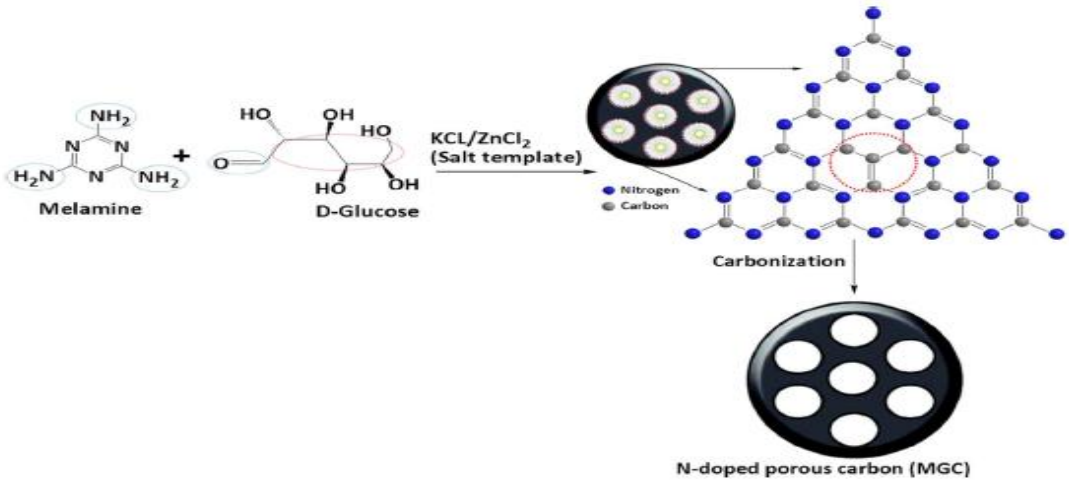

Figure 2.42 Synthesis scheme of N-doped porous carbon (132)

The (133) has prepared porous carbon by combining tin tetrachloride and sodium polyacrylate in a ratio of 5:14, using a template method. The average particle size of the porous carbon is 21 µm. The paraffin was loaded in the porous carbon to develop shape stabilized PCM which was tested for thermo-physical properties. The results suggest that the composite PCM was chemically stable and have 35 J/g of latent heat storage capacity. Additionally, the shape stabilized PCM has shown good thermal stability and durability.

2.3.3 Graphite schaffolds

The graphite is the crystalline form of carbon with a hexagonal structure. It is one of the stable forms of carbon under standard conditions and is available in both synthetic and natural forms. The most common form of graphite used to provide shape stability to the

PCM is expanded graphite (EG). EG is a modified form of graphite that has a layered structure with interlayer space (134). It is prepared by the oxidation of graphite in the presence of sulfuric acid and nitric acid. Table 2.9 shows the thermo-physical properties of EG. It has good thermal conductivity and can expand up to 150-200 times.

Table 2.9 Thermo-physical properties of EG (135)

Parameter	Value
Thermal conductivity (W/mK)	150
Bulk density (kg/m^3)	120
Carbon content (%)	98
Average pore size (nm)	80

Figure 2.43 shows the SEM image of expanded graphite. It can be visualized that EG has a honeycomb sub-structure with numerous pores of diamond shapes. The size of these diamond shape pores varies from 0.6 µm-3.0 µm. The EG has been widely used to improve the thermal characteristics of the PCM (136) and to overcome the limitation of leakage.

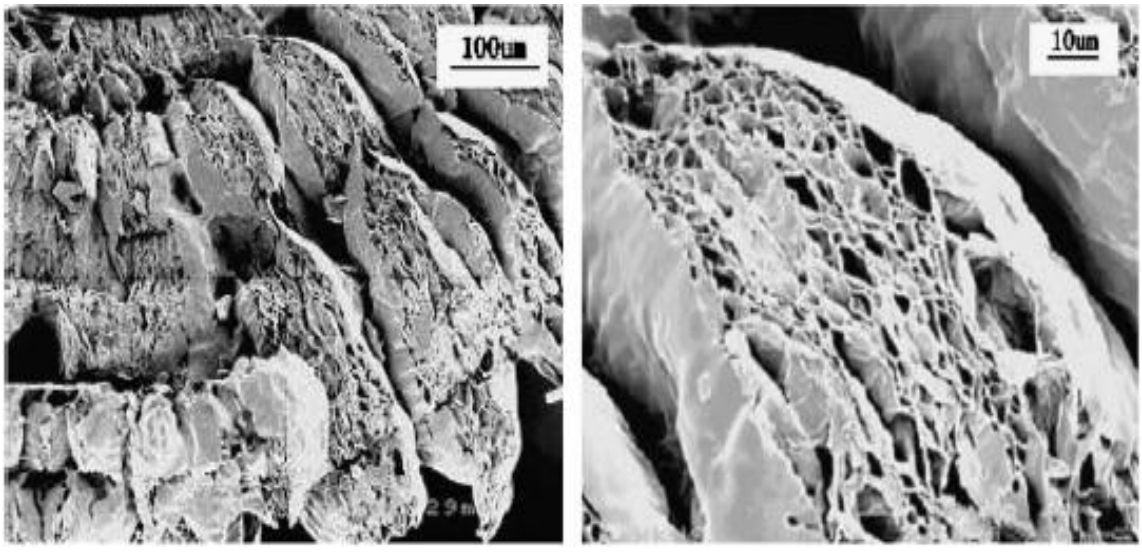

Figure 2.43 SEM images of expanded graphite with different magnification (137)

Various studies have shown the application of EG to improve the thermal conductivity of shape stabilized PCM. Table 2.10 shows summary of studies that investigated the effect on the thermal characteristics of organic PCM to prepare shape stabilized composite PCM. In these studies, the EG is directly impregnated in organic PCM to improve the thermal conductivity and reduce the leakage of the composite PCM. It has been found that the enhancement in the thermal conductivity of the composite PCM is sharp in comparison to the parent organic PCM. There are various studies where EG was used to enhance the thermal conductivity of the mixture of PCM along with supporting porous material like bentonite (138), diatomite (139), expanded perlite (140) (141) and others.

Table 2.10 Summary of studies published using EG as supporting material

Weight percentage of EG	PCM	Impregnation method	Latent heat, H (kJ/kg)	Thermal reliability (thermal cycles)	Thermal conductivity enhancement	Ref.
7.2 wt% EG	Myristic-Palmitic - stearic acid	Microwave treatment	153.5	1000	From 0.25 to 2.51 W/mK	(142)
12 wt% EG	Stearic-Benzamide acid	Direct impregnation	176.03	100	12.30 times	(143)
7 wt% EG	Tetradecanol	Autoclave method	202.6	-	5.37 times	(144)
5.3 wt% EG	Lauric-Myristic-Palmitic acid	Adsorption method	135.9	50	From 0.21 to 1.67 W/mK	(145)
10 wt% EG	Capric-palmitic-stearic acid	Adsorption method	131.7	500	From 0.3407 to 1.125 W/mK	(146)
10 wt% EG	Stearic acid	Vacuum impregnation	169.90	1000	-	(147)
25 wt% EG	Stearic acid	Direct impregnation	154.0	10	130 times	(148)
10 wt% EG	Erythritol	Impregnation and sintering	212.5	140	17.38 times	(149)
10 wt% EG	PEG	Adsorption method	108.1	-	19.4 times	(150)
20 wt% EG	Paraffin (RT100)	Absorption	163.6	200	0.665 to 6.8 W/mK	(151)
30 wt% EG	Octadecane	Vacuum impregnation	159.9	-	-	(152)

2.3.4 Polyurethane foam

Polyurethane foam (PUF) is a cross-linked polymer with an open cell and closed cell structure. These cellular materials are developed by reaction of polyols with iso-cyanates in the presence of catalysts, additives, and blowing agents. PUF is widely used as an insulating material because of its lower thermal conductivity, excellent thermal insulating properties, chemically stable, and low cost (153). PUF is an efficient absorbent because of its hydrophobic nature (154) therefore, PUF is widely explored to contain the PCM and reduce the leakage as shown by the SEM image in Figure 2.44. Taking the advantage of the thermal energy storage capacity of the organic PCM and excellent insulating property of PUF, the combination of these two is widely explored in the field of thermal energy storage in the buildings for improving building energy efficiency (155). Numerous studies have reported that PUF-PCM shows good thermal, chemical, and physical properties along with high durability for the application of thermal energy storage (156) (157).

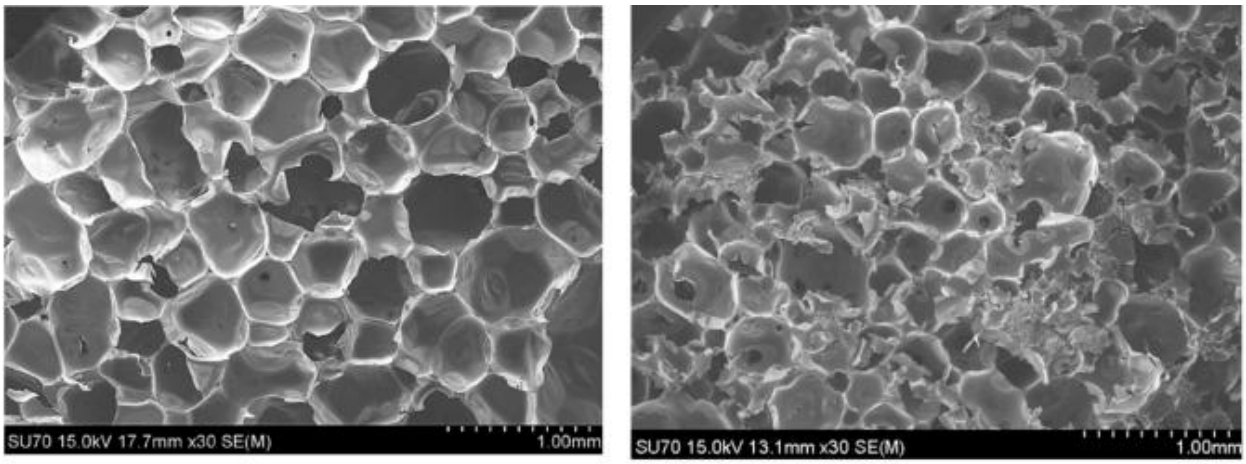

Figure 2.44 SEM images of (a) Raw PUF (b) PUF with PCM (157)

The (158) has prepared a crosslinked polyurethane copolymer using 2-hydroxypropyl-b-cyclodextrin as a chain extender and PEG as a soft segment. The prepared

polyurethane copolymer was then used as a matrix material to load PEG and form a shape stabilized PCM, with a dual-phase transition, as shown in Figure 2.55. The results show that the maximum loading of 60 wt% of PEG was achieved without leakage in shape stabilized PCM. Due to the dual-phase transition i.e. solid-liquid (because of PEG) and solid-solid (because of polyurethane matrix) the shape stabilized PCM shows higher heat storage density compare to other traditional shape stabilized PCM. Thermal cycling and TG analysis suggest that the shape stabilized PCM has good reliability and thermal stability respectively.

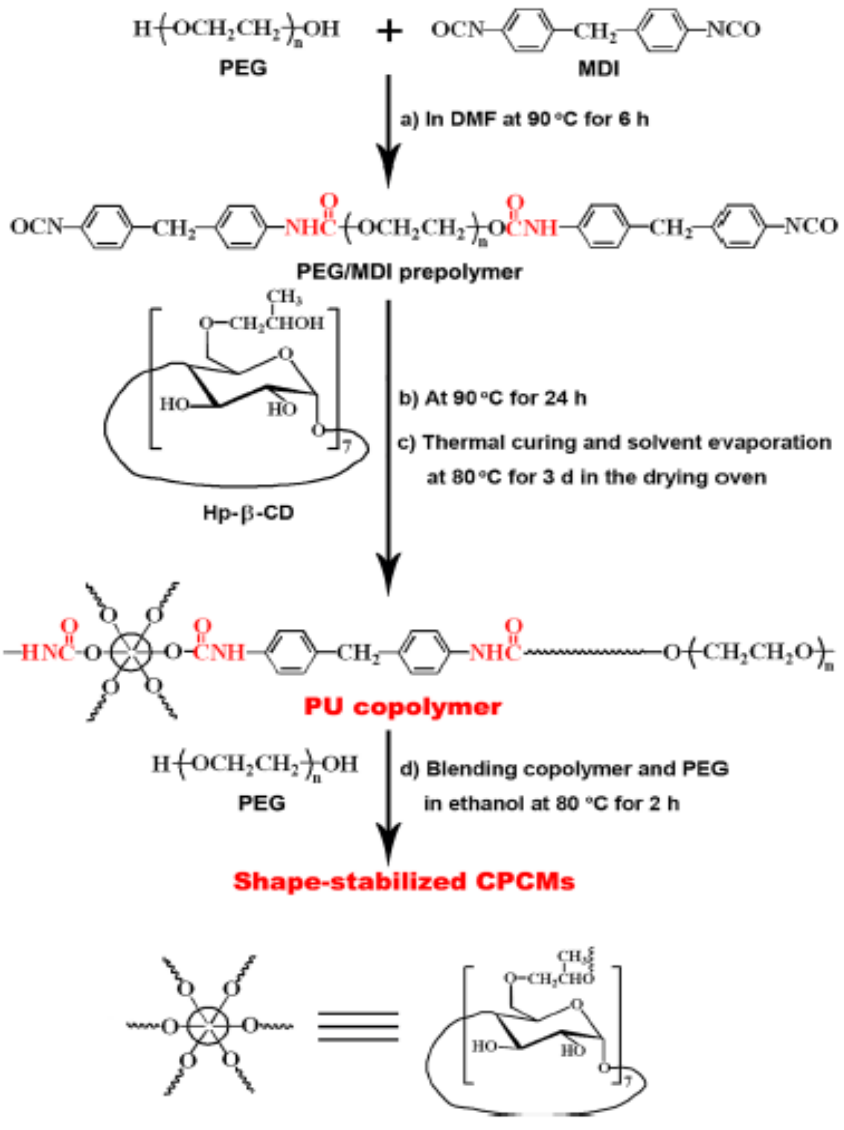

Figure 2.55 Scheme of preparation of shape stabilized PCM using polyurethane (158)

The (159) has prepared PEG-based polyurethane, wood powder and, GO shape stabilized composite PCM, as shown in Figure 2.56, and performed the characterization to evaluate solar thermal energy storage properties. The wood powder was mixed in an aqueous solution of GO and then PEG was mixed in this mixture, stirred, and undergoes thermal curing at 80 °C. Prepared sample with 80 wt% of polyurethane-based on PEG, 19.2 wt% of wood powder and 0.8 wt% of GO have shown high thermal conductivity of value 1.87 W/mK along with melting latent heat capacity of 140.2 J/g and freezing latent heat capacity of 139.4 J/g. The reliability test revealed that there is no significant reduction in the latent heat capacity of the shape stabilized composite PCM.

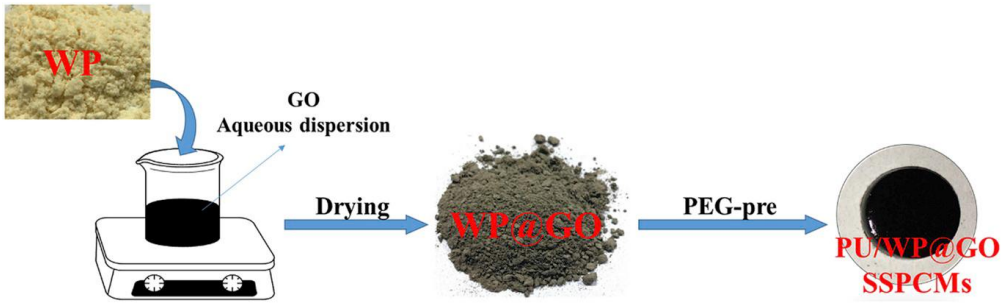

Figure 2.56 Preparation procedure of Polyurethane/wood powder/GO based shape stabilized composite PCM (159)

A novel work has been reported by (160) who prepare a shape stabilize PCM using hexadeconal as PCM and dye-polyurethane as porous supporting material as shown in Figure 2.57. The dye-polyurethane was prepared through step condensation under the nitrogen atmosphere using PEG10000 and distilled toluene. The hexadeconal was mixed in a specific concentration of dye polyurethane and was vacuum evaporated and dried. The DSC results show two different peaks, one of hexadeconal phase change and the other of dye-polyurethane phase change. Thus, this composite can effectively regulate the temperature because of two different phase transition temperatures. The highest phase change enthalpy

of 229.5 J/g was shown by the sample carrying 63.8% of dye-polyurethane in the composite along with peak transition temperature of 39.6 °C and 50.3 °C. The TG analysis shows that the composite is thermally stable at working temperature.

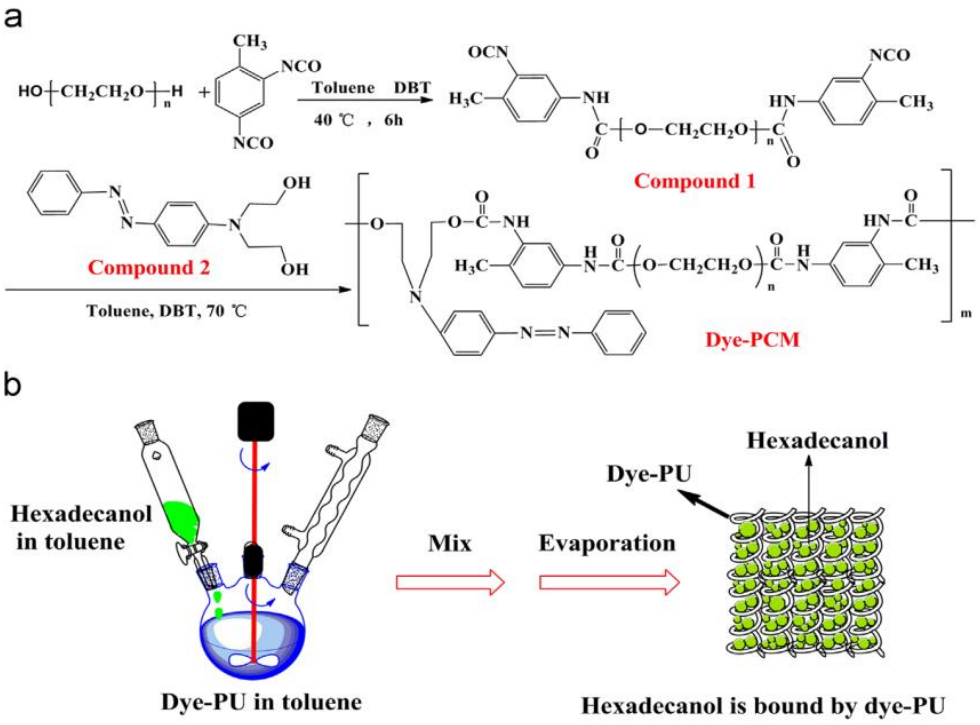

Figure 2.57 Schematic of preparation of dye-polyurethane/hexadeconal shape stabilized PCM (160)

2.3.5 Silica scafollds

Silica is a highly porous material with a low density and a large internal surface area. Its 3-D network structure prevents the leakage of the PCM during the phase transition. Silica fumes have good compressive, tensile, and flexural strength and thus it can be used as a replacement of concrete in building materials (161). The high porosity of silicon dioxide has been investigated by many researchers to develop shape stabilized composite PCM. The (162) developed PEG/SiO_2 composite PCM and found that the maximum percentage of PEG loading in SiO_2 without any leakage is 85%. It also exhibits a large enthalpy of 162.9 J/g.

Similarly, (163) has developed PEG/SiO_2 shape stabilized PCM with varying PEG mass fraction, viz. 30%, 40%, 50%, 60%, 70%, and 80%, using sol-gel method. The latent heat of storage of PEG (80%)/ SiO_2 is 128.4 J/g and its thermal conductivity is 0.279 W/mK. The study also shows that the thermal conductivity of PEG(80%)/ SiO_2 was enhanced from 0.279 to 0.558 W/mK by adding 2.7% mass fraction of graphite.

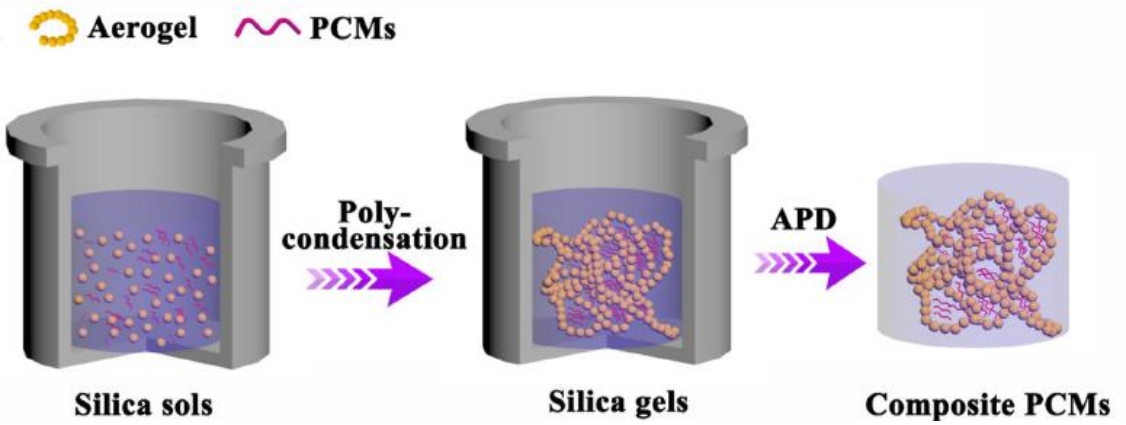

Figure 2.58 In situ one-step preparation of monolithic silica aerogel based composite PCM (164)

The (164) has developed monolithic silica aerogel-based composite PCM for efficient thermal energy storage through in-situ one-step strategy as shown in Figure 2.58. The developed sample has shown good hydrophobicity with contact angle 124° and a latent heat storage capacity of 127.73 J/g along with 0.12 W/mK of thermal conductivity. The (165) has used dried flexible silica aerogel for the development of monolithic shape-stabilized composite PCM which exhibits high loading amount of PCM, increased energy storage, and improved thermal conductivity. The shape stabilized composite PCM has exhibited 70% loading of the PCM without any leakage along with 122.7 J/g of latent heat storage and good thermal stability. The (166) has developed various silica/paraffin shape stabilized composite PCM through the solution impregnation method as shown in Figure 2.59. Mesoporous silica and two different forms of diatomite were used as skeleton material.

The organic PCM has well preserved in the pores and was held by capillary force and interfacial interaction. It is analyzed that the shape stabilized PCM preserves its stability even after 1000 thermal cycles and 30 days melting. The mesoporous silica with PCM mass fraction of 60% has shown enthalpy of 95 J/g.

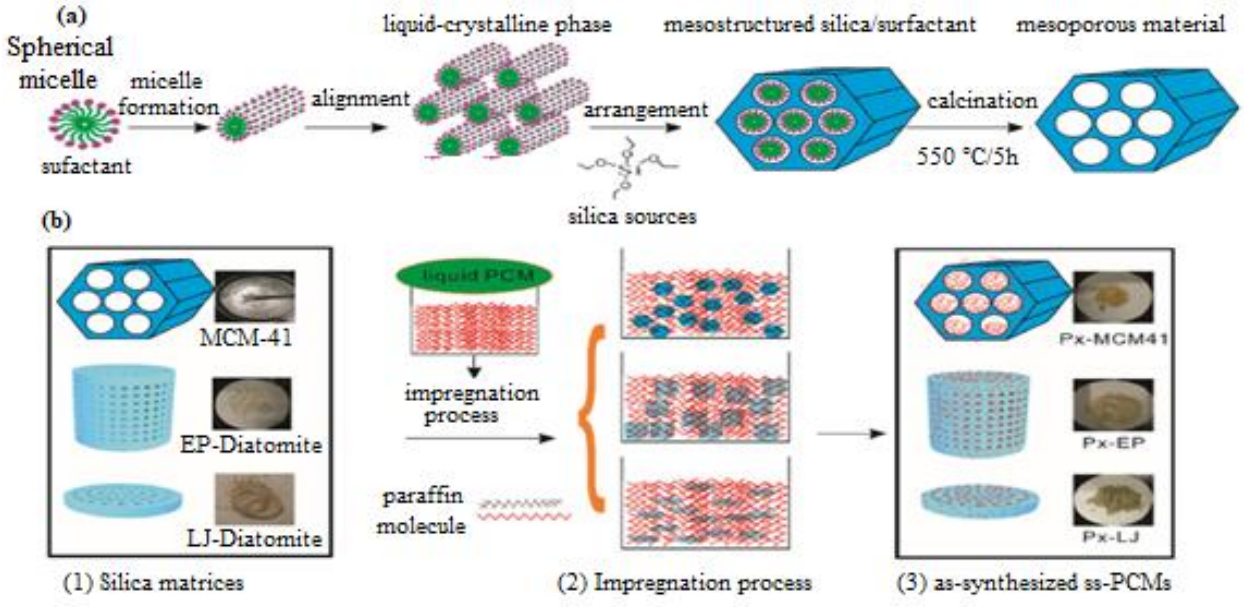

Figure 2.59 Scheme of preparation of shape stabilized composite PCM using mesoporous silica and two different diatomite (166)

Silicon dioxide was used to improve the shape stability of the paraffin (RT 28 from rubitherm) impregnated by EG (167) using sol-gel method. The mass fraction of silicon dioxide and EG is 20.8% and 7.2% in the form-stable composite PCM respectively. The result shows an enhancement of 94.7% in the thermal conductivity of the composite PCM in comparison to paraffin. Consequently, there is a reduction in heating and cooling time of the composite PCM. The composite PCM has a latent heat capacity of 104.4 J/g. Nano SiO_2 was used as supporting material for a ternary eutectic mixture of Capric-Palmitic-Stearic acid to develop form stable composite PCM (57). 75% of the CA-PA-SA was impregnated into nano SiO_2 through the adsorption method. The study measured 99.43 J/g of latent heat

capacity of the composite PCM which reduces to 94.29 J/g after 500 thermal cycles. The low thermal conductivity of the nano SiO_2 leads to a reduction in the thermal conductivity of the composite PCM, from 0.3407 W/mK to 0.08239 W/mK in comparison to ternary eutectic mixture of organic PCM. The (168) has prepared LA/SiO_2 shape stabilized PCM through a facile one-pot method involving co-hydrolysis and co-condensation process as shown in Figure 2.60. LA is confined in the nanopores of SiO_2 with an effective mass percentage of 36.4%, 49.9%, 52.4%, and 56.6% with the corresponding latent heat of 60.3, 82.7, 86.9, and 93.8 J/g respectively. After 600 thermal cycles, the latent heat storage of 56.6% LA/SiO_2 and 49.9 % LA/SiO_2 is 93.4 and 82.6 J/g respectively. This shows that the prepared shape stabilized PCM is thermally stable.

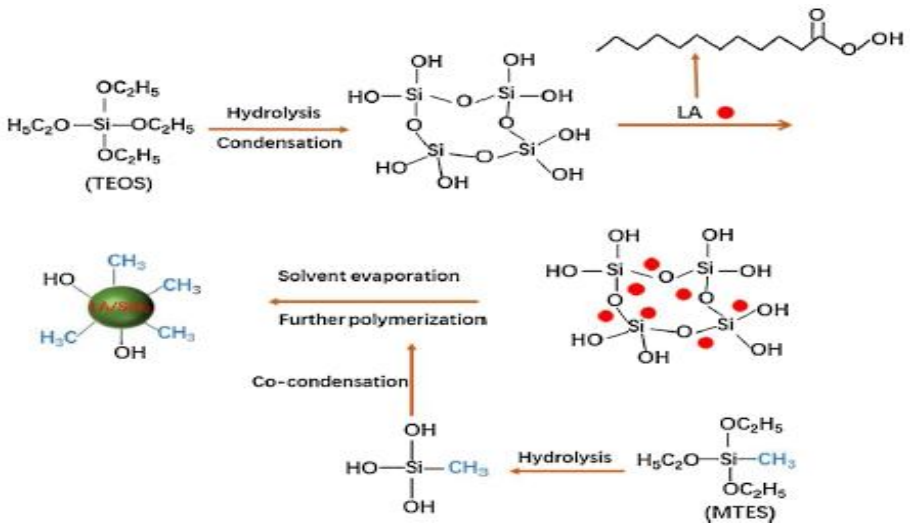

Figure 2.60 One pot method for preparation of LA/SiO_2 shape stabilized PCM (168)

2.3.6 Clays

The clay mineral-based materials have excellent porosity and large specific surface area. Thus, they can easily withhold the PCM and provides excellent shape stabilization. The clay mineral-based materials have the advantage of substantial reserves and moderate cost. However, the low thermal conductivity of clay minerals is one of the constrain to use for

building applications in comparison to other supporting materials like expanded graphite. Therefore, to overcome this demerit, nano-particles are also loaded along with PCM and clay mineral-based material to prepare shape stabilized composite PCM for building applications. The methods used for the preparation of clay/PCM based shape stabilized PCM include vacuum impregnation, melting intercalation, melting adsorption, and variations (169). Enhanced thermal conductivity and reduced leakage are the two major advantages of embedding organic PCM in clay material and nanoparticles .

Table 2.11 Composition of clay materials used for preparation of shape stabilized PCM

	SiO_2	**Al_2O_3**	**Fe_2O_3**	**CaO**	**MgO**	**K_2O**	**H_2O**	**Etc.**	**Ref.**
Diatomite	57.4	15.9	9.1	0.6	9.0	3.3	1.8	0.2	(170)
Expanded perlite	73.6	12.4	1.25	0.91	0.15	4.18	4.35	3.16	(171)
Expanded vermiculite	38.0-46.0	10.0-16.0	6.0-13.0	1.0-5.0	16.0-35.0	1.0-6.0	8.0-16.0	-	(172)
Bentonite	61.82	17.3	3.0	4.5	2.1	1.24	-	-	(173)
Kaolin	57.63	37.76	0.86	0.346	0.596	1.801	-	0.91	(174)
Sepiolite	51.95	2.14	0.41	2.77	23.35	0.36	-	19.02	(122)

Table 2.11 shows the composition of commonly used clay-based material for the development of shape stabilized composite PCM. Enhanced thermal conductivity of the shape stabilized composite PCM will increase the heat transfer rate thereby reducing the time for solidifying and liquefying of the PCM. Reduced leakage will ensure proper stability of the PCM and high loading of the PCM (approx up to 86%) in clay and thereby enhancing the latent heat storage capacity of the shape stabilized composite PCM. Table 2.12 summarizes various studies on the thermal characterization of shape stabilized composite

PCM using clay mineral-based material. However, because of the crystal formation of the PCM within the clay, the heat storage capacity of the shape stabilized PCM is lower in comparison to the organic PCM. The most commonly used clay materials, which provide stability to the PCM, are diatomite, expanded perlite, vermiculite, kaolin, bentonite, etc.

Table 2.12 Summary of published literature on thermal characterization of shape stabilized PCM using clays

Porous Material	PCM	Loading percentage	Imprignation method	Latent heat, H (kJ/kg)	Thermal reliabity (Thermal cycles)	Thermal conductivity, λ (W/mK)	Ref.
Diatomite	n-hexadecane	50	Vacuum impregnation	120.1	-	-	(175)
Diatomite	n-octadecane	50	Vacuum impregnation	116.8	-	-	(175)
Diatomite	Paraffin wax	50	Vacuum impregnation	61.96	-	-	(175)
Raw diatomite	Paraffin mixture	39.13	Magnetic stirring	41.26	-	-	(176)
Calcined Diatomite	Paraffin mixture	50.62	Magnetic stirring	56.40	-	-	(176)
Diatomite	Capric acid/Lauric acid	53.6	Vacuum impregnation	87.33	-	0.219	(177)
Diatomite	PEG	50	Vacuum impregnation	87.09	200	0.32	(178)
Diatomite	Paraffin	32	Direct impregnation	53.15	400	-	(179)
Diatomite	Stearic acid and palmitic acid	65.2	Vacuum impregnation	106.7	100	-	(180)
Diatomite	Palmitic acid and capric acid	66.6	Magnetic stirring	104.0	-	0.119	(181)
Diatomite	PEG	58	Vacuum impregnation	105.70	200	-	(182)
Diatomite	Stearic acid	40	Direct impregnation	57.1	-	-	(183)
Hybradized diatomite	Myristic acid	72	Vacuum impregnation	124.3	200	0.58	(184)

Microwaved modified diatomite	Lauric acid	40	Direct impregnation	49.7	-	-	(185)
Diatomite	Capric acid	50	Direct impregnation	78.9	120	-	(186)
Expanded perlite	Paraffin	50	Vacuum impregnation	60.9	-	-	(187)
Expanded perlite	Octadecane	59.35		132.2	-	0.2310	(170)
Expanded perlite	Lauric acid	70	Direct mixing	105.58	100	-	(188)
Expanded perlite	Capric acid and stearic acid	50	Physical attraction	82.1	1000	-	(189)
Expanded perlite	Paraffin	60	Direct impregnation	80.9	2000	-	(190)
Expanded perlite	Lauric-palmitic-stearic acid	55	Vacuum impregnation	81.5	1000	0.44	(191)
Expanded vermiculite	Stearic acid	-	Vacuum impregnation	77.6	-	0.52	(192)
Acid treated expanded vermiculite	Stearic acid	-	Vacuum impregnation	116.0	-	0.48	(192)
Expanded vermiculite	Capric and lauric acid	57.48	Vacuum impregnation	81.34	200	0.135	(193)
Modified expanded vermiculite	Stearic acid	63.12	Vacuum impregnation	134.31	200	0.52	(194)
Expanded vermiculite	Paraffin	64.6	Vacuum impregnation	126.19	-	0.154	(195)
Expanded vermiculite	Lauric acid	60	Vacuum impregnation	126.8	200	0.28	(196)
Expanded vermiculite	Octadecane	80.65	-	142.0	-	0.1569	(170)
Modified expanded vermiculite	Capric-stearic-myristic acid	86.4	Vacuum impregnation	86.4	200	0.667	(197)
Bentonite	Capric acid	40	Vacuum impregnation	74.08	1000	0.43	(173)
Bentonite	PEG600	43	Vacuum impregnation	56.72	1000	0.39	(173)
Bentonite	Dodecanol	32	Vacuum impregnation	67.55	1000	0.48	(173)
Bentonite	Heptadecane	18	Vacuum impregnation	38.42	1000	0.35	(173)

Bentonite	Paraffin	44.4	Solution intercalation	39.84	10	-	(198)
Bentonite	Myristic acid	50	Vacuum impregnation	53.3	5	0.32	(199)
Kaolin	Paraffin	60	Vacuum impregnation	119.49	-	0.413	(200)
Kaolin	Capric acid	17.5	Vacuum impregnation	27.23	1000	0.17	(201)
Kaolin	PEG 600	21	Vacuum impregnation	32.80	1000	0.18	(201)
Kaolin	Heptadecane	16.5	Vacuum impregnation	34.63	1000	0.20	(201)
Hybrid Kaolin	Stearic acid	-	Vacuum impregnation	66.30	200	-	(202)
Boron nitride	Bio-based PCM	80	Vacuum impregnation	117.6	30	0.729	(203)
Sepiolite	Lauric acid	60	Vacuum impregnation	125.2	200	0.59	(204)
Sepiolite	Paraffin	36.93	Direct impregnation	62.08	-	-	(205)
Sepiolite	Deconic acid	21.68	Direct impregnation	35.69	-	-	(205)

2.3.7 Nano-particles

Nanoparticles are the materials that are confined to the nanoscale. These materials have a particle size of less than 100 nm, have a very high surface-to-volume ratio, and have excellent thermal conductivity. Therefore, nanoparticles are widely used in TES systems (206) to enhance the thermal conductivity of the PCM (207,208). For example, organic PCM possess low thermal conductivity because of which their application in TES is limited. Therefore, nanoparticles can act as a catalyst for the organic PCM to improve their heat transfer rate. Table 7 summarizes the thermal conductivity, density and 3-dimensional structure of commonly used nanoparticles in shape stabilized composite PCM. It can be seen in the Table 2.13 that nanoparticles have excellent thermal conductivity due to which they are commonly used to enhance the heat transfer rate of a material. There are various factors on which thermal conductivity enhancement of shape stabilized PCM loaded with

nanoparticles depends like the concentration of nanoparticles, Brownian motion, clustering of nanoparticles, purity, aspect ratio, interfacial thermal resistance, and intermolecular interaction (209).

Table 2.13 Thermo-physical properties of nanoparticles used to prepare shape stabilized organic PCM (209–217)

S.No.	Nanomaterial	Thermal conductivity (W/mk)	Density (kg/m^3)	3-Dimensional structure
1	(a) SWCNT (b) MWCNT	3000	2600	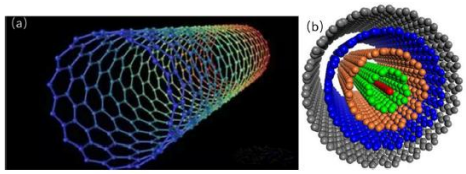
2	GO	3000	3600	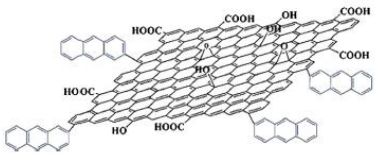
3	CNF	4000	2260	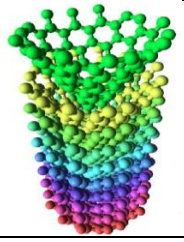
4	Al_2O_3	40	3970	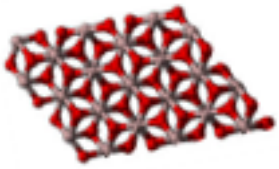
5	Ag	429	10500	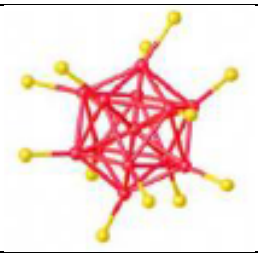

6	xGNP	1500	2200	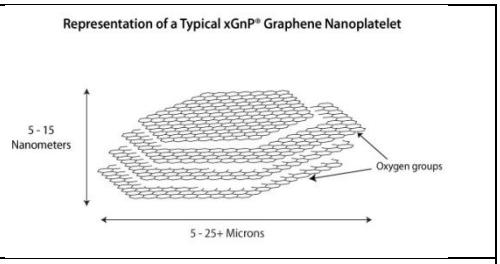
7	TiO_2	8.4	4250	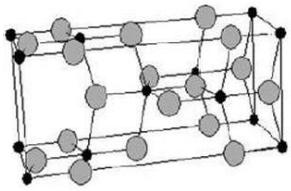
8	ZnO	23.4	5606	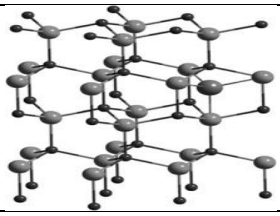

A summary of previously published studies on thermal properties enhancement of shape stabilized PCM loaded with nanoparticles is shown in Table 2.14. This table summarizes a list of nanoparticle, PCMs and supporting materials used to prepare shape stabilized composite PCM. Additionally, it also shows the content of PCM (in wt%) in shape stabilized composite PCM, thermal conductivity and latent heat content of composite PCM. Commonly used nanomaterials to enhance the heat transfer rate of the organic PCM are Cu, Ag, CNT, Al_2O_3, GnP, nano graphite, CNF, TiO_2, graphene, and ZnO. The techniques used to impregnate the nanoparticles in the organic PCM are vacuum impregnation, varnish layer, kneader mixing technique, sonication and ultrasonication, stirring and sonication, and autoclave method (209).

Table 2.14 Summary of published literature on thermal properties of shape stabilized PCM loaded with nanoparticles

Nanoparticle	PCM	Supporting material	Particle fraction in PCM (wt%)	Thermal conductivity (W/mK)	Latent heat (kJ/kg)	Ref.
HNT@Ag	PEG1000	-	3.3 wt%	0.9023	71.3	(43)
			1.3 wt%	0.73	72.5	
Cu	PEG6000	SiO_2	0.51 wt%	0.337	121.4	(218)
			2.1 wt%	0.414	110.2	
			3.9 wt%	0.426	100.4	
xGnP	Bio-based PCM	-	1 wt%	0.274	146.6	(219)
			3 wt%	0.612	144.5	
			5 wt%	0.670	143.5	
CNT	Bio-based PCM	-	1 wt%	0.410	133.4	(219)
			3 wt%	0.490	132.4	
			5 wt%	0.536	130.1	
Nano graphite	Paraffin	-	1 wt%	0.365	202.58	(220)
			4 wt%	0.497	193.26	
			7 wt%	0.568	183.62	
			10 wt%	0.936	181.81	
Graphene oxide	Paraffin	-	-	0.985	63.76	(221)
AgNP	PEG	Diatomite	7.2 wt%	0.82	111.3	(222)
CNT	n-eicosane	Expanded Perlite	0.3 wt%	0.19	160.38	(223)
			0.5 wt%	0.24	159.02	
			1 wt%	0.32	157.43	
Al_2O_3	PEG	SiO_2	3.3 wt%	0.398	122.0	(224)
			9.2 wt%	0.419	107.8	
			12.6 wt%	0.435	123.8	
xGnP	Hexadecane	Diatomite	-	0.419	120.8	(225)
	Octadecane	Diatomite	-	0.351	126.1	
	Paraffin	Diatomite	-	0.412	63.77	
MWCNT	Paraffin (RT20)	-	0.15 wt%	~ 0.15	137.20	(226)
			0.30 wt%	~ 0.16	127.28	
			0.45 wt%	~ 0.18	129.50	
			0.60 wt%	~ 0.21	133.60	
MWCNT	Paraffin	Diatomite	0.26 wt%	1.70	89.40	(227)
TiO_2	Lauric-stearic acid	-	1.0 wt%	0.27	173.22	(228)
ZnO		-	1.0 wt%	0.29	173.64	
CuO		-	1.0 wt%	0.32	173.86	
GnP	Myristic acid	-	1 wt%	0.230	189.19	(229)
			2 wt%	0.267	187.39	
			3 wt%	0.294	187.19	
MWCNT	Myristic acid	-	1 wt%	0.191	191.99	(229)
			2 wt%	0.202	190.12	
			3 wt%	0.208	188.47	
Nano graphite	Myristic acid	-	1 wt%	0.189	191.27	
			2 wt%	0.195	190.67	
			3 wt%	0.205	188.90	

MWCNT	Octadecane-HDPE	4 wt% EG	1 wt%	1.36	-	(230)
		3 wt% EG	2 wt%	1.09	-	
CNF		4 wt% EG	1 wt%	1.03	-	(230)
S-MWCNT	Paraffin Wax	-	5 wt%	0.324	178.22	(231)
L-MWCNT		-	5 wt%	0.309	177.39	
CNF		-	5 wt%	0.305	185.05	
GNP		-	5 wt%	0.7	186.50	
MWCNT	n-octadecane	5 wt% EG	0 wt%	0.85	171.10	(232)
		4 wt% EG	1 wt%	1.36	170.45	
		3 wt% EG	2 wt%	1.09	168.27	
		2.5 wt% EG	2.5 wt%	0.71	168.79	
		0 wt% EG	5 wt%	0.52	170.16	
CNF	n-octadecane	5 wt% EG	0 wt%	0.85	171.10	(232)
		4 wt% EG	1 wt%	1.03	168.37	
		3 wt% EG	2 wt%	0.96	166.34	
		2.5 wt% EG	2.5 wt%	0.54	167.29	
		0 wt% EG	5 wt%	0.37	169.38	
CNT	PEG	41 wt% Diatomite	0 wt%	0.15	51.43	(233)
			0.57 wt%	0.26	53.79	
			1.70 wt%	0.27	55.89	
SWCNT	PEG	Diatomite	2.0 wt%	0.87	109.8	(234)
MWCNT	PEG	SiO_2	0 wt%	0.359	102.8	
			0.5 wt%	0.389	139.4	
			1 wt%	0.421	139.6	
			2 wt%	0.444	133.8	
			3 wt%	0.463	135.1	
GNP	PEG	GO	4 wt%	1.72	167.4	(235)
		-	4 wt%	1.61	167.5	
Cu nanowires	Tetradeconal	-	58.9 wt%	2.86	86.95	(236)
GO	PEG	13.6 wt% Boron nitride	1.5 wt%	0.85	160.8	(237)
		14.4 wt%	0.8 wt%	1.06	164.1	
GO sheets	PEG	-	4 wt%	-	142.8	(238)
Cu nano wire	Paraffin	-	1.95 wt%	0.280	173.2	(239)
TiO_2	30 % n-octadecane	-	-	0.45	44.2	(240)
	40%	-	-	0.42	69.2	
	50%	-	-	0.38	85.8	
	60%	-	-	0.35	119.8	
GO	PEG	-	4 wt%	-	174.5	(241)
Graphene dopped with nitrogen	Palmitic acid	-	1 wt%	0.34	199.65	(242)
		-	2 wt%	0.46	198.84	
		-	3 wt%	0.98	199.48	
		-	4 wt%	1.54	197.53	
		-	5 wt%	1.73	195.54	
GNP-300 m^2/g	Palmitic acid	-	22.01 wt%	2.75	160.31	(243)
GNP-500 m^2/g		-	16.94 wt%	2.43	170.72	
GNP-750 m^2/g		-	8.26 wt%	2.11	188.98	

MWCNT	Beeswax	-	5 wt%	0.46	115.5	(244)
			20 wt%	0.58	91.6	
xGNP	Coconut oil	-		1.33	82.34	(36)
	Palm oil			1.26	77.18	
MWCNT	Stearic acid	-	1 wt%	~0.44	196.0	(245)
		-	5 wt%	0.47	185.3-188.6	
Graphene		-	1 wt%	~0.39	191.5	
		-	5 wt%	0.54	185.3-188.6	
Graphite		-	1 wt%	~0.78	199.3	
		-	5 wt%	3.2	185.3-188.6	
CNT	Myristic acid	Silica fume	0.3 wt%	0.35	89.57	(246)
			0.5 wt%	0.39	88.76	
			1.0 wt%	0.46	87.43	

2.3.8 Applications of shape stabilized PCM in buildings

The enhanced thermal conductivity, negligible leakage, and substantial thermal energy storage capacity has made shape stabilized PCM as one of the prominent materials for improving building energy efficiency. Therefore, various studies have been conducted in the recent past to evaluate the effect of shape stabilized PCM for improving indoor thermal behavior of the buildings. The (247) has prepared ceremsite-based shape stabilized PCM and embedded it in concrete to analyze the thermo-physical properties of the concrete. The shape stabilized PCM consists of LA-SA/Al_2O_3/Cermasite (LA-SA/Al_2O_3/C). The optimum quantity of LA-SA/Al_2O_3 is 82 wt% LA+18 wt% SA+0.5 wt% Al_2O_3. This LA-SA/Al_2O_3 has a latent heat storage capacity of 205.9 kJ/kg and thermal conductivity of 0.2843 W/mK. The shape stabilized PCM was impregnated in the concrete, with a varying mass fraction of 0%, 3%, 6%, 10%, 15%, and 20%, to develop concrete-based CPCM blocks as shown in Figure 2.61 (a) of sizes 10×10×2 cm and 10×10×3 cm. The testing of the developed concrete-based CPCM blocks was done in an incubator as shown in Figure 2.61 (b). The measured results revealed that the temperature of the hot side and cold side of the concrete-based CPCM block is lower in comparison to normal concrete block. Additionally, an

increase in delay time was also observed in the composite block compare to a normal block. An increase in the thickness of the concrete-based CPCM will increase the thermal energy storage performance.

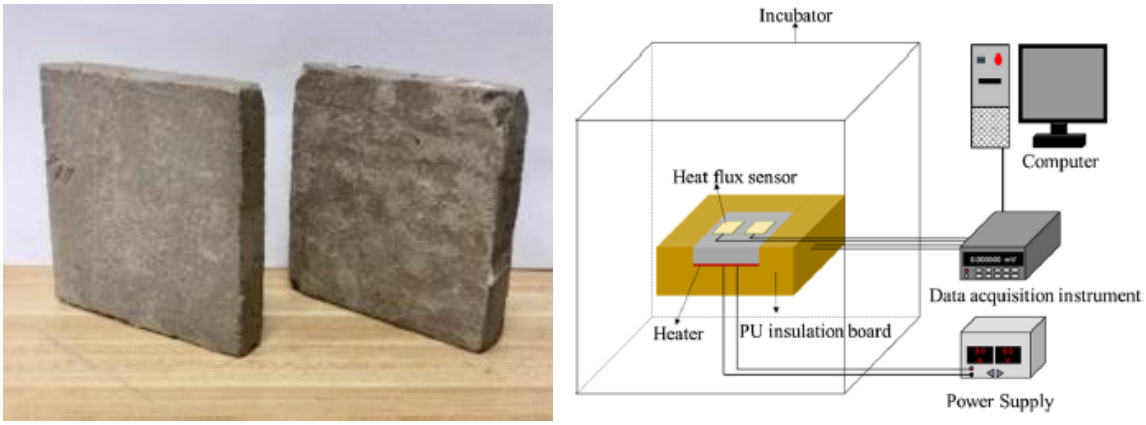

Figure 2.61 (a) Normal concrete block (left) concrete-based CPCM block (right) (b) Experimental setup for thermal performance of the concrete blocks (247)

The (248) has used ss-PCM sheets, as shown in Figure 2.62, made of hexadecane-octadecane and supported by polypropylene and elastomer for shape stability. These ss-PCM sheets were used in three identical huts to evaluate the effect of indoor thermal behavior. Hut A does not have any ss-PCM sheet, hut B has ss-PCM sheet in the floor and hut C has ss-PCM sheet on the floor, wall, and ceiling.

Figure 2.62 Shape stabilized PCM sheets (248)

The results suggest that in hut B and C the heat absorbance and heat released were increased by 23.6% and 25.5% respectively. Additionally, it was also reported that the consumption of heater in hut B and C was reduced by 9.2% and 18.4% in comparison to hut A.

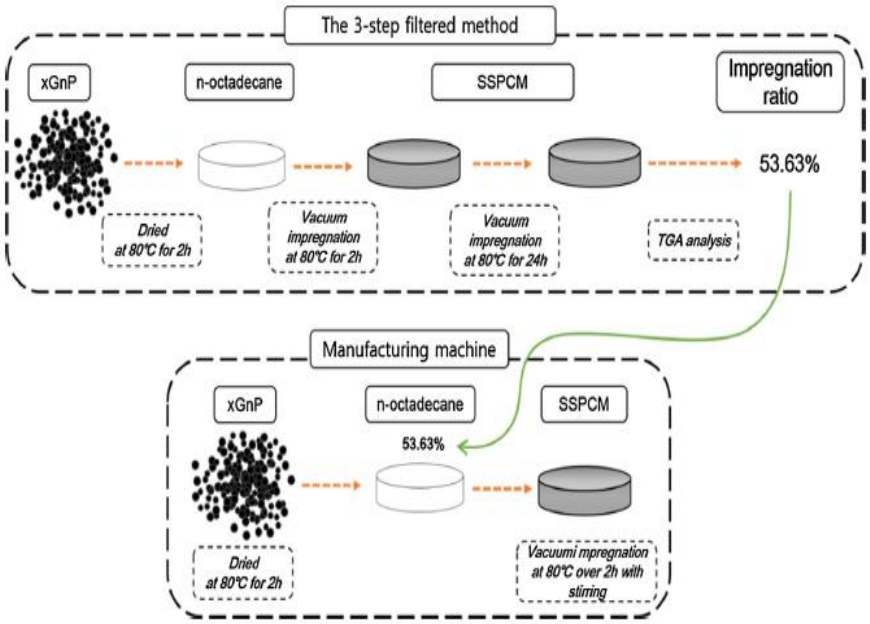

(a)

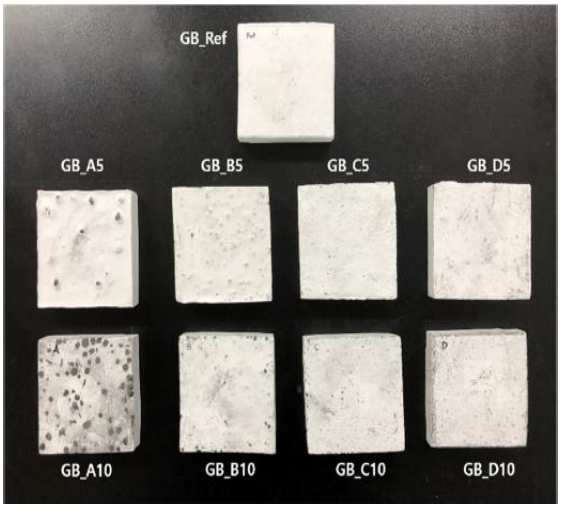

(b)

Figure 2.63 (a) Preparation of shape stabilized composite PCM (b) Developed gypsum board/shape stabilized composite PCM (249)

The (249) has developed shape stabilized PCM using n-octadecane as PCM and xGnP as nanoparticles and applied it in gypsum board as shown in Figure 2.63. Figure 2.63 (a) shows the scheme of preparation of shape stabilized PCM and Figure 2.63 (b) shows developed gypsum board embedded with shape stabilized PCM. A detailed dynamic thermo-graphic analysis and dynamic heat flow analysis was conducted along with energy and cooling energy consumption using energyPlus8.5. The gypsum board with shape stabilized composite PCM stores more thermal energy in comparison to the reference gypsum board. Additionally, cooling energy reduction of 3.4% was achieved by adding 10% shape stabilized PCM in gypsum board.

The (250) has developed shape stabilized PCM (SSPCM) using n-octadecane as a PCM an EV and EP as porous clay supporting material and impregnate it in Red Clay (RC) to develop RC-shape stabilized PCM panels. The panels were prepared by varying the weight percentage of shape stabilized PCM developed using EP (EP-SSPCM) and EV (EV-SSPCM) in RC. The developed panels contains 2.5 wt%, 5 wt%, 7.5 wt%, 10 wt% of EP-SSPCM and 2.5 wt%, 5 wt%, 7.5 wt%, 10 wt% of EV-SSPCM. These panels were then tested for thermal behavior in climate cycling test using chamber as shown in Figure 2.64. The results depict a highest time lag of 1.33 hours by 10 wt% EP-SSPCM panel and lowest time lag of 0.15 hour by 2.5 wt% of both EP-SSPCM and EV-SSPCM panel. Highest peak temperature reduction up to 1.6 °C achieved by 10 wt% EP-SSPCM panel and lowest peak temperature reduction was measured for 2.5 wt% of EP-SSPCM panel.

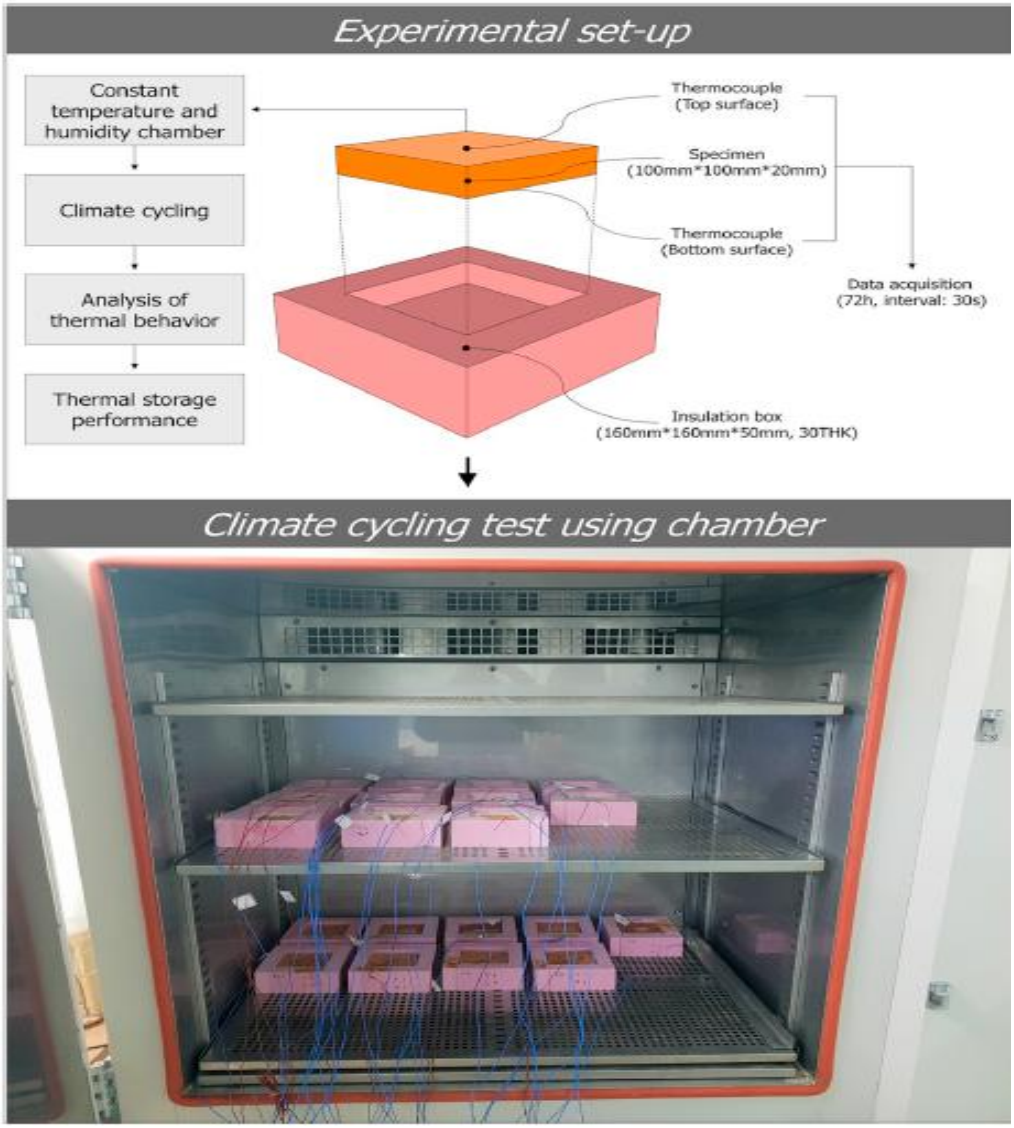

Figure 2.64 Experimental setup of climate cycling test chamber (250)

The (251) has prepare shape stabilized PCM using paraffin wax, HDPE and EG to incorporated it in cement mortar for developing PCM bricks. Two similar walls of dimensions 1.5 m × 1.5 m were developed and tested in a thermal chamber. One wall is developed using shape stabilized PCM bricks while the other was developed using regular vitrified bricks as shown in Figure 2.65. The results suggest that the heat storage capacity of the PCM wall with 120 mm thickness was 12.7% and 61% higher than that of regular wall

of thickness 240 mm in the temperature range of 15 °C – 30 °C and 18 °C – 24 °C respectively. The author suggests that the PCM wall is not suitable to use in summer and in winter season. However, The PCM wall shows excellent thermal response under mid-season cases. Additionally, significant evaporative leakage was also observed during the test.

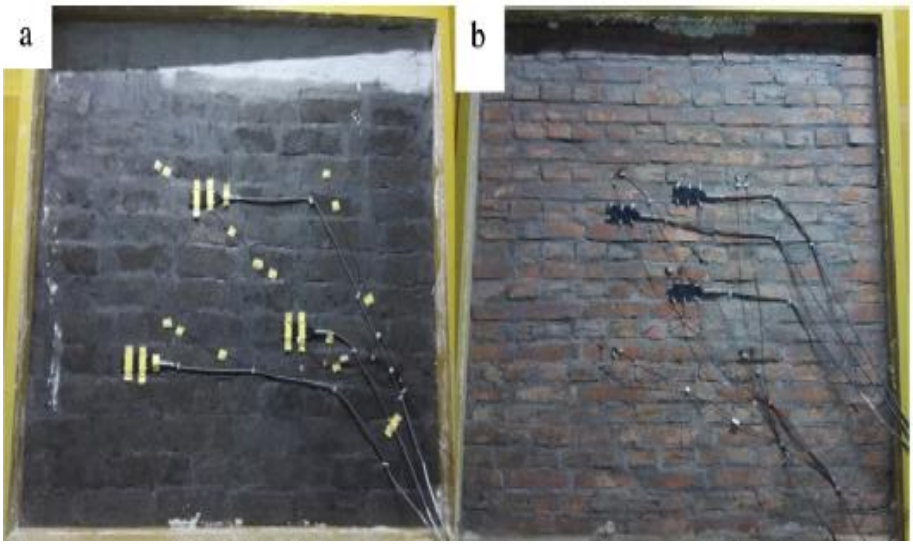

Figure 2.65 Developed (a) PCM wall using shape stabilized PCM bricks (b) Regular wall (251)

The (252) has prepared shape stabilized PCM using octadecane as PCM and xGnP as supporting material and mixed with concrete, as shown in Figure 2.66, to investigate the effect of various mix proportions on mechanical and thermal properties of the developed concrete. The thermal result shows that the thermal conductivity of the concrete loaded with shape stabilized PCM varies from 1.97 W/mK to 1.6 W/mK whereas regular concrete have 2.01 W/mK of thermal conductivity. The conductivity of the concrete loaded with shape stabilized PCM decreases with increase in the content of shape stabilized PCM. However, the specific heat of the concrete increases with increase in shape stabilized PCM content in the temperature range of 10 °C to 24 °C.

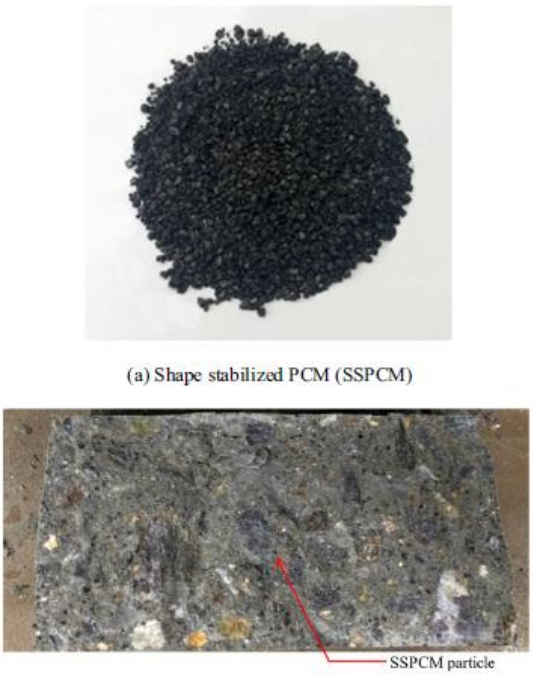

Figure 2.66 (a) Shape stabilized PCM (b) Concrete loaded with shape stabilized PCM (252)

A novel shape stabilized PCM was developed by (253) using bio-based PEG and wood flour (WF) through vacuum adsorption method. Two types of wood flour are used viz. high length-to-diameter ratio (HWF) and low-length-to diameter ratio (LWF). The maximum enthalpy of 137.0 J/g was shown by PEG4000/30 wt% HWF. The study suggests that the adsorption performance of HWF is better than LWF in shape stabilized PCM. The maximum loading percentage of of PEG1000, PEG4000 and PEG10000 was 75 wt%, 70 wt%, and 70 wt% in HWF shape stabilized PCM respectively.

The (51) has developed a novel shape stabilized PCM wallboard using paraffin as PCM and EP as supporting porous material and installed it in a test room, as shown in Figure 2.67 (a), (b) and (c), to evaluate the indoor thermal performance both numerically and experimentally. The latent heat storage capacity of PCM wallboard is 67.13 J/g and 69.06 J/g for melting and freezing process respectively. The results revealed that the PCM room attained reduction in maximum temperature of 2.13 K, 3.4 K, 2.13 K, 2.96 K, and 2.04

K on first, second, third, fourth and fifth day respectively. However, the average minimum peak temperature of the PCM test room is 2.29 K higher than test room without PCM. The one dimensional numerical model was integrated with TRNSYS software and was well validated with the experimental data. The numerical study shows that the PCM wallboard can effectively reduce the average temperature of an office building during two months of summer by 9.22 K between operational time of 7:00-18:00.

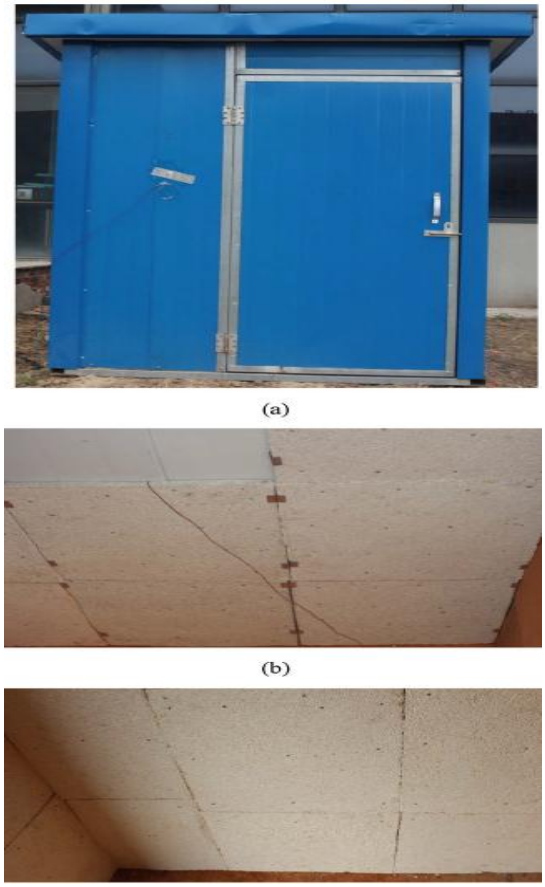

Figure 2.67 (a) Test room photograph (b) Wallboard with shape stabilized PCM on the roof (c) Wallboard with shape stabilized PCM on the wall (51)

The (254) has developed double layered shape stabilized PCM wallboard made of 80% of paraffin, 15% of HDPE and 5% of EG. The shape stabilized PCM wallboard was then placed on south wall of the test room called as PCM room and a comparative analysis on

indoor thermal behavior was conducted, with a similar test room which is without shape stabilized PCM wallboard as shown in Figure 2.68 (a). The schematic of the shape stabilized PCM wallboard placed on the south wall of the PCM room is shown in Figure 2.68 (b).

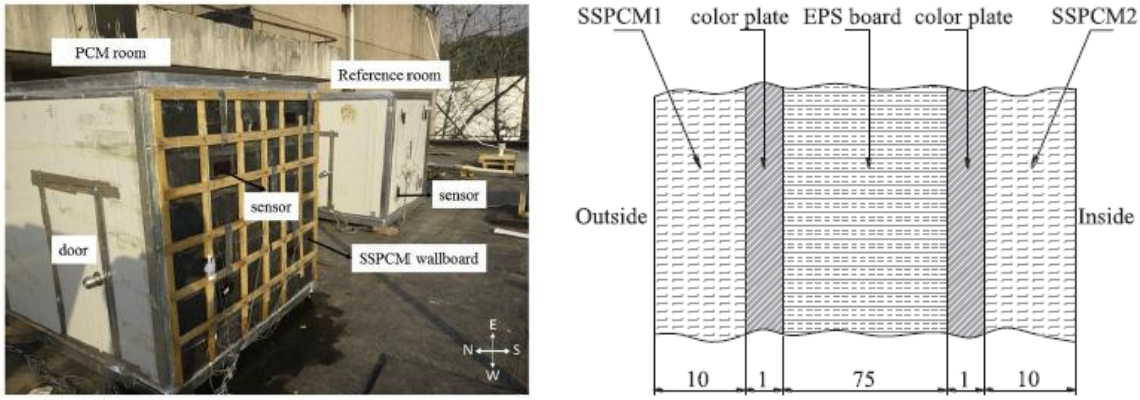

(a) (b)

Figure 2.68 (a) PCM room and Reference room (b) Schematic of the south wall with shape stabilized PCM wallboard (254)

Following results has been revealed:

- The indoor wall temperature of the PCM room was 2.4 °C lower in maximal and 0.5 °C lower in average during summer in comparison to reference room.
- The indoor air temperature of the PCM room was 1.9 °C lower in maximal and 0.6 °C lower in average then reference room during summer.
- During winter the indoor surface wall temperature of the PCM room was 1.6 °C higher in maximal and 0.1 °C higher in average compare to the reference room.
- In winter the indoor air temperature of the PCM room is 1.3 °C lower in maximal and 0.1 °C higher in average compare to the reference room.
- The heat flux test suggest that in summer the PCM wallboard absorb more heat from the indoor air during day and releases it during night. However, in winter the

wallboard absorb more heat from outdoor air during daytime and released it during night.

The (255) has developed a thermal energy storage composite material using diatomite shape stabilized paraffin as PCM and wood-flour/HDPE (WF/HDPE) as matrix. Various samples were developed by varying the wt% of stabilized PCM, wood-flour and HDPE. The result shows that the developed thermal energy storage composite has overcome the leakage problem because of the presence of WF/HDPE. The composite is chemically and thermally stable and possess considerable thermal energy storage capacity along with temperature regulating ability. A similar work has also been reported by (256), where EG supported PCM was used along with wood flour/HDPE as matrix to prepare shape stabilized PCM. The following claims have been made: (a) PCM shows excellent stability in EG because of the presence of small pores in EG. (b) The maximum latent heat capacity of 39.04 J/g has been shown by the sample containing 30 wt% of EG supported PCM, 28 wt% of wood flour, and 42 wt% of HDPE. The measured thermal conductivity of this sample is 0.235 W/mK. (c) The thermal reliability test suggests that after 500 thermal cycles the reduction in melting and solidifying latent heat was 25.0% and 23.0% respectively.

The (257) has developed form stabilized composite PCM by infiltrating Sepiolite (SEP) in a fatty acid eutectic mixture of capric acid and stearic acid (FAEM) through direct impregnation technique and temperature regulation test by mixing it with cement -based plaster was conducted at laboratory scale as shown in Figure 2.69. The developed stabilized PCM of SEP/FEAM (40%) has shown a latent heat storage capacity of 76.16 J/g at a melting temperature of 22.86 °C. Moreover, after 1000 thermal cycles the latent heat and melting point were reduced to 69.86 J/g and 22.81 °C respectively. The result shows an increase in the time lag of the control room in comparison to the test room. Additionally, the indoor

temperature of the control room was reduced to 2.07 °C for reasonable heating time duration.

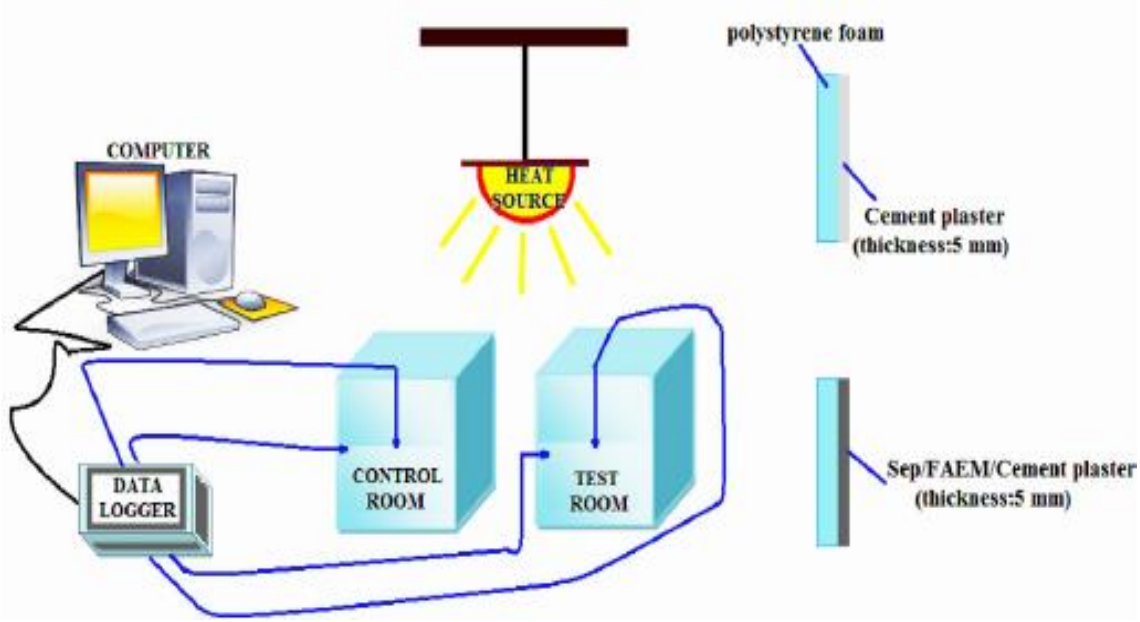

Figure 2.69 Experimental setup for evaluating the temperature regulating performance of SEP/FEAM/Cement plaster (257)

The (258) has done a performance evaluation of shape stabilized PCM made of paraffin wax as PCM and graphite foam as supporting material using the Energy Saving Index (ESI) as an evaluation index. The shape stabilized PCM was used as a plate of dimensions 290 mm × 290 mm × 25 mm. Two identical test rooms were developed, one is with shape stabilized PCM plates and the other is without PCM plates. The results suggest that the shape stabilized PCM plate could improve the indoor thermal performance of the building structure by lowering down the temperature fluctuations and indoor temperature decline rate. The (44) has developed a shape stabilized PCM using dodecanol as a PCM and diatomite as supporting material. Furthermore, this composite PCM was mix with cement-lime plaster to analyze the phase change behavior of the composite plaster mixture. It was found that the melting and freezing latent heat values are 4.88 J/g and 4.37 J/g for 8 wt% of

shape stabilized PCM in cement plaster and 10.32 J/g and 9.87 J/g for 16 wt% of shape stabilized PCM in cement plaster. Additionally, the enthalpy of the modified plaster is proportional to the amount of shape stabilized PCM added.

The (259) has developed PCM bricks of dimensions 240 mm × 120 mm × 90 mm using shape stabilized PCM to evaluate the thermal performance of the building enclosure. The shape stabilized PCM is made of 70 wt% paraffin wax, 15 wt% EG, and 15 wt% HDPE. The shape stabilized PCM bricks were used to develop a wall of a real size room of dimension 3.25 m × 3.86 m × 2.91 m as shown in Figure 2.70. The tested wall has dimensions 1.60 m × 2.40 m × 0.24 m and it faces northwest direction. The results suggest that in the midseason day more indoor comfort environment is created along with a time lag of 2-3 hours. In the summer season, the situation becomes critical because the PCM remains in liquid form all the time and therefore the wall shows poor thermal performance in summer season. In the summer season maximum values of temperature and heat flow are higher for the shape stabilized PCM wall in both free-floating and air conditioning cases.

Figure 2.70 Images of tested room (a) South view (b) Tested wall (c) Indoor view (259)

The (260) has proposed the improvement in the thermal behavior of hollow concrete floor panel of dimension 28 cm × 28 cm × 3.75 cm, as shown in Figure 2.71 , by inserting shape stabilized PCM made of 85 wt% of paraffin wax as a PCM and 15 wt% of SBS polymer as supporting material. The latent heat of melting of paraffin was 110 J/g at a melting temperature of 27 °C. The results show an enhanced time lag of almost 3.7 hours compare to the panel without PCM. The variation in temperature and values of temperature are reduced compare to the panel without PCM.

Figure 2.71 Image of hollow concrete panel (260)

The (261) has prepared three different walls having different shapes of shape stabilized PCM as shown in Figure 2.72. The shape stabilized PCM was integrated using direct mixing and lamination interpolation method. The thermal performance of these walls was compared with an ordinary wall. The shape stabilized PCM was made off paraffin mixture and HDPE. The latent heat storage capacity thermal conductivity and melting temperature of the shape stabilized PCM are 160.3 J/g, 0.099 W/mK, and 24.9°C respectively. Each of these three walls contains mass percentage of 10% of shape stabilized PCM. The analysis suggests that the surface temperature and heat flow in the PCM wall is less compare to the ordinary wall. Also, the energy saving is better in the wall prepared using lamination interpolation method compare to the wall prepared through direct mixing.

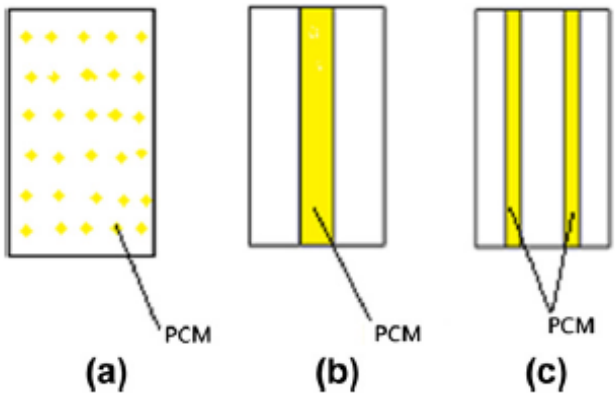

Figure 2.72 Shape stabilized PCM location in the wall (261)

The (38) has prepared a shape stabilized PCM by impregnating octadecabe in xGNP through vacuum impregnation method. Maximum 55.9% of octadecane was impregnated in xGNP and has a thermal energy storage capacity of 110.9 J/g. The octadecane/xGNP shape stabilized PCM was then mix with cement mortar having cement mass content of 10 wt%, 20 wt% and 30 wt% for evaluating the thermal performance of the prepared composite.

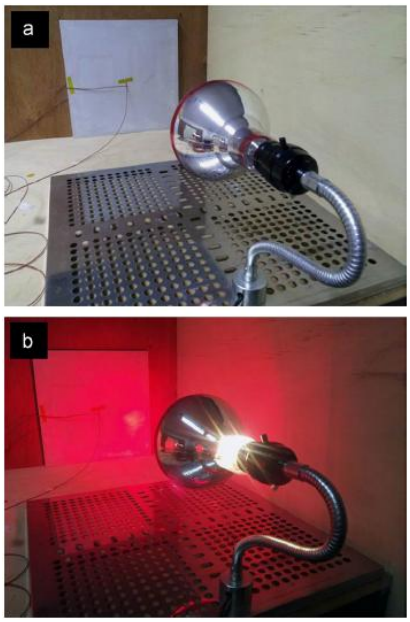

Figure 2.73 Shape stabilized PCM location in the wall (38)

The experimental setup was shown in Figure 2.73 which consists of a wall made of plywood panel and rock wool having a heat source of infrared radiation lamp of 250 W. The

results have shown increment in the thermal conductivity of the octadecane/xGNP/cement composite by increasing the content of octadecan/xGNP shape stabilized PCM content. The octadecane/xGNP/cement has shown a very effective time lag along with high heat transfer rate.

The (262) has done theoretical and experimental study by preparing high conduction shape stabilized PCM made of paraffin(solid and liquid)/HDPE/Expanded graphite and utilizing it in under floor heating system of a test house to provide space heating as shown in Figure 2.74. The size of the test room 4 × 3 × 3 m and is located on the second floor of a sub-tropical climate where annual average temperature is 15.4 °C. Adjacent to the test room a similar room was used to compare the performance of shape stabilized PCM room with conventional room. For robust result comparison a conventional heating air-conditioner was also introduces in the experimental setup. The floor temperature of the phase change system varies cyclically and the floor surface temperature is always higher than the indoor temperature. Additionally, the phase change system is more economical among different kind of heating system.

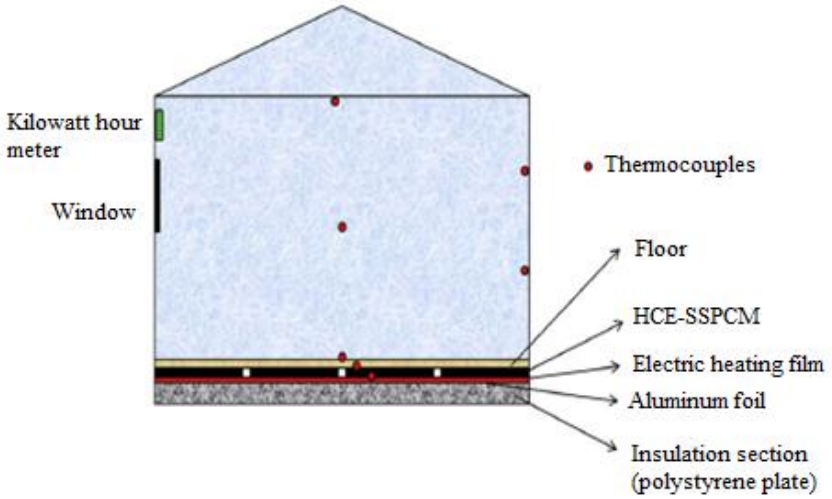

Figure 2.74 Schematic of under floor heating system (262)

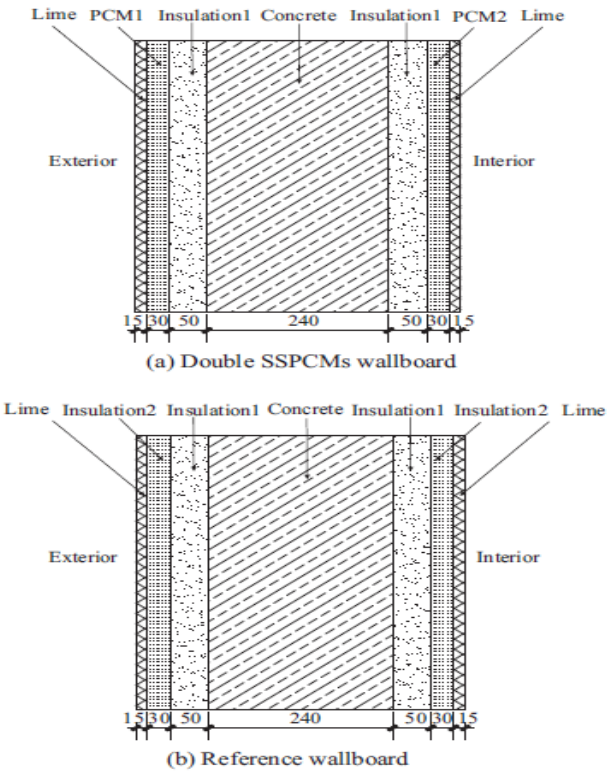

Figure 2.75 Proposed double layer shape stabilized PCM wallboard (b) Reference wallboard without shape stabilized PCM (263)

The (263) has developed a novel sandwich-type wallboard having a three-layer panel as shown in Figure 2.75. The internal and external layer of the wallboard has shape stabilized PCM and the middle layer consist of cement. The shape stabilized PCM consists of paraffin (80 wt%) as PCM and HDPE 15 wt%/EG 5 wt% as supporting material. Two test room, one with shape stabilized PCM wallboard and the other without shape stabilized PCM wallboard, of dimensions 9 m × 5 m × 3 m were proposed to evaluate the effect of shape stabilized PCM wallboard mounted with constant and variable frequency air conditioner by the numerical study. The outer layer of the wallboard is active in the hot season while the inner layer is active in the cold season. The results suggest that the variable frequency air-conditioned room having shape stabilized PCM wallboard consumes 6.4% and 17.8% less energy compare to the reference room during summer and winter respectively. The shape

stabilized PCM wallboard room reduces the heat gain in summer daytime and heat loss in winter daytime compare to the reference room in air-conditioned buildings. Overall, the variable frequency air conditioner room with shape stabilized PCM wallboard exhibits better performance in both the season compared to the reference room.

The (264) has used CFD numerical investigation to evaluate the effect of incorporating the shape stabilized PCM in the outer layer of the roof of a building. The shape stabilized PCM compose of paraffin with mass ratio of 85% and HDPE with a mass ratio of 15%. The results revealed that the decrement factor of the roof with PCM is 85% lower than that of the roof without PCM. The peak temperature of the inner surface of the roof is also decreased by over 3.7 °C. The (265) has used a dynamic energy simulation program to investigate the effect of using 22 different shape stabilized PCM in improving the low heat storage capacity of wooden building structure along with reducing building energy consumption. The analysis shows that there is an average reduction of 5% in annual energy consumption along with a reduction of 4.1 °C in peak temperature in summer was achieved by using shape stabilized PCM. The (266) has evaluated numerically, the thermal characteristic of shape stabilized PCM wallboard with a sinusoidal temperature wave on the outer surface. Additionally, the performance of shape stabilized PCM wallboard was compared with brick, foam concrete, and expanded polystyrene. The result suggests that the PCM wallboard shows a distinct characteristic compare to brick, foam cement, and expanded polystyrene.

Based on the literature review of methods of incorporation of PCM in the building envelope to improve the indoor thermal behavior of the building, a comparative analysis of various characteristics of microencapsulation, macroencapsulation and shape-stabilized PCM was shown in Table 2.15. It has been analyzed that macroencapsulation technique has major advantages of low cost, ease in manufacturing, high reliability, high durability,

availability in various shapes and sizes, and low physical damage during mixing or loading in concrete. Therefore, based on these findings, further study was conducted on evaluating the effect of embedding PCM using macroencapsulation method in building envelope to investigate the effect in indoor thermal behavior of the building in the tropical climate of India.

Table 2.15 Comparative analysis of various methods of incorporating PCM in building envelope

	mPCM	**MPCM**	**ss-CPCM**
Latent heat storage capacity	Increased	Increased	Increased
Capability of regulating indoor temperature	High	High	High
Cooling load reduction capability	High	High	High
Thermal conductivity	Reduced	Not affected	Increased
Compressive strength	Reduced	Reduced	Reduced
Chances of damage	High	Very low	Low
Cost	High	Less	High
Manufacturing techniques	Typical	Easy	Typical
Applicability in building material other than concrete	Less	High	High
Availability in various shapes	No	Yes	Yes
Customized fabrication	No	Yes	Yes
Ease in handling	No	Yes	No
Durability	Low	High	Low
Reliability	Low	High	Low